

High Spatial Order Energy Stable FDTD Methods for Maxwell's Equations in Nonlinear Optical Media in One Dimension

Vrushali A. Bokil¹ · Yingda Cheng² · Yan Jiang² ·
Fengyan Li³ · Puttha Sakkaplangkul²

Received: 17 November 2017 / Revised: 22 March 2018 / Accepted: 17 April 2018
© Springer Science+Business Media, LLC, part of Springer Nature 2018

Abstract In this paper, we consider electromagnetic (EM) wave propagation in nonlinear optical media in one spatial dimension. We model the EM wave propagation by the time-dependent Maxwell's equations coupled with a system of nonlinear ordinary differential equations (ODEs) for the response of the medium to the EM waves. The nonlinearity in the ODEs describes the instantaneous electronic Kerr response and the residual Raman molecular vibrational response. The ODEs also include the single resonance linear Lorentz dispersion. For such model, we will design and analyze fully discrete finite difference time domain (FDTD) methods that have arbitrary (even) order in space and second order in time. It is challenging to achieve provable stability for fully discrete methods, and this depends on the choices of temporal discretizations of the nonlinear terms. In Bokil et al. (J Comput Phys 350:420–452, 2017), we proposed novel modifications of second-order leap-frog and trapezoidal temporal schemes in the context of discontinuous Galerkin methods to discretize the nonlinear terms in this Maxwell model. Here, we continue this work by developing

Research is supported by NSF Grant DMS-1720116. Research is supported by NSF Grants DMS-1453661 and DMS-1720023. Research is supported by NSF Grant DMS-1719942.

✉ Puttha Sakkaplangkul
sakkapla@math.msu.edu

Vrushali A. Bokil
bokilv@math.oregonstate.edu

Yingda Cheng
ycheng@math.msu.edu

Yan Jiang
jiangyan@math.msu.edu

Fengyan Li
lif@rpi.edu

¹ Department of Mathematics, Oregon State University, Corvallis, OR 97331, USA

² Department of Mathematics, Michigan State University, East Lansing, MI 48824, USA

³ Department of Mathematical Sciences, Rensselaer Polytechnic Institute, Troy, NY 12180, USA

similar time discretizations within the framework of FDTD methods. More specifically, we design fully discrete modified leap-frog FDTD methods which are proved to be stable under appropriate CFL conditions. These method can be viewed as an extension of the Yee-FDTD scheme to this nonlinear Maxwell model. We also design fully discrete trapezoidal FDTD methods which are proved to be unconditionally stable. The performance of the fully discrete FDTD methods are demonstrated through numerical experiments involving kink, antikink waves and third harmonic generation in soliton propagation.

Keywords Maxwell's equations · Nonlinear dispersion · High order FDTD · Energy stability · Soliton propagation

1 Introduction

Optics and photonics research focuses on phenomenon involving multiple scales, and simulating the full Maxwell partial differential equation (PDE) models to adequately capture useful optical effects is important. Numerical simulation of EM pulse propagation in nonlinear optical materials can be achieved by solving the full Maxwell equations along with models that adequately capture the response of the medium. One way to model this response is by appending to Maxwell's equations systems of ordinary differential equations (ODEs) for the dynamic evolution of the electric polarization which depends nonlinearly on the electric field. This method is called the *auxiliary differential equation* (ADE) technique [17, 18, 23, 26]. In this paper we use the ADE technique to model EM wave propagation in a nonlinear optical material in which the electric polarization comprises of three responses; a linear response modeled by a single-pole Lorentz dispersion, a nonlinear instantaneous response governed by the Kerr effect and a nonlinear retarded response (nonlinear dispersion) due to Raman scattering [1]. The linear Lorentz, Kerr and Raman nonlinearities are idealized phenomenological models that we choose because of their widespread applicability to modeling the response of a variety of nonlinear materials [56].

Among a variety of numerical methods that have been developed for EM wave propagation in nonlinear materials, the finite difference time domain (FDTD) method developed by Kane Yee in 1969, called the Yee scheme [49], is the most popular FDTD scheme for computing numerical solutions of time dependent EM problems. The original Yee scheme was developed for EM wave propagation in a vacuum (linear medium). This scheme discretizes the time-dependent Maxwell's equations on a staggered space–time grid resulting in a second order accurate method in space and time, which is nondissipative but dispersive [44]. The Yee scheme has been extended to linear dispersive media [23, 27, 28] (in particular see the books [44, 45] and references therein), and then to nonlinear dispersive media [17, 19, 23, 43, 56]. In addition to the ADE technique, other methods that model the material responses have been developed, one example being the recursive convolution methods [29, 37, 38, 53] for linear dispersive materials. Additional references for Yee and other FDTD methods for EM wave propagation in linear and nonlinear Lorentz dispersion can be found in [7, 18, 24, 25, 42] for the 1D case, and in [13, 26, 56] for 2D and 3D cases. In recent years, extensions of the second order Yee-FDTD technique to higher order discretizations have also been considered. Several higher order formulations of the FDTD method have been analyzed for the case of linear media [4, 40, 41, 48, 50, 52, 54]. In [16], a fourth order FDTD method coupled to a second order leap frog time integrator is used to analyze nonlinear optical materials.

Other numerical approaches for EM wave propagation have also been constructed in the literature. Low order finite element methods (FEM) [32–34], and high order discontinuous

Galerkin (DG) methods [14,20–22,31,47,55] have been developed for the simulation of Maxwell's equations in linear dispersive media and meta-materials [35]. The FEMs model complex geometries better than the FDTD methods. However, FEMs have not been well developed for the nonlinear Maxwell models that we consider in this paper. FEM analysis for a nonlinear Maxwell model can be found in [10]. In [46], the authors construct a pseudospectral spatial domain (PSSD) approach for linear Lorentz dispersion and nonlinear Kerr response. In [30], the PSSD method is used to numerically study optical carrier wave shock. Additionally, Finite Volume (FV) based methods for nonlinear Kerr media are constructed in [3,9]. Here, the Maxwell-Kerr model is written as a hyperbolic system and approximated by a Godunov scheme in [3], and a third order Roe solver in [9].

In [5], we presented for the first time in the literature, energy results for the nonlinear Maxwell model with linear Lorentz, Kerr and Raman responses in one spatial dimension. Based on these energy results we have presented the construction and analysis of high order DG methods in space along with appropriate temporal discretizations that result in fully discrete energy stable DG methods. We believe that ours is the first paper to present energy identities for this nonlinear model and design numerical (DG) methods whose discrete energy relations mimic the energy relations of the nonlinear model. As the main contribution of this work, we proposed a novel strategy to discretize the nonlinear terms within the commonly used leap-frog and implicit trapezoidal temporal discretization. The resulting fully discrete leap-frog DG and trapezoidal DG methods are proved to be stable. More specifically, the modified leap-frog DG method is conditionally stable under an expected CFL condition, while the modified trapezoidal DG method is unconditionally stable. In both cases, we discretize the ODE part of the model system implicitly.

Given the popularity and importance of FDTD methods in the computational electromagnetics community, in this paper, we continue our work by presenting the construction of high spatial order FDTD methods for the nonlinear Maxwell model in one dimension. We construct fully discrete FDTD methods by employing appropriate temporal discretizations that *obey discrete versions of the energy relations of the nonlinear Maxwell model*. We would like to point out, that this is the first paper considering the construction of fully discrete FDTD methods that preserve important physical properties (energy decay or conservation), and thus provide *compatible* discretizations for the nonlinear Maxwell model under consideration. Performing such constructions in one spatial dimension is important in understanding how to *mimic* important conservation laws in a simple setting before considering the full three spatial dimensional model.

Using the ADE technique, we focus on a first order formulation of the nonlinear Maxwell model in one spatial dimension. This model includes Maxwell's equations written as a system of first order PDEs along with a system of first order ODEs that model the material response. We discuss the construction of explicit and implicit FDTD methods which are second order accurate in time and $2M$ order accurate in space for $M \in \mathbb{N}$. As in our previous work in [5], the time discretizations are based on leap-frog and trapezoidal time integrators that are carefully modified so that the fully discrete leap-frog and trapezoidal FDTD methods are energy stable. The lowest order fully discrete leap-frog FDTD method can be viewed as an extension of the Yee scheme [49] to the nonlinear Maxwell model, while the lowest order trapezoidal FDTD method is an extension of the Crank–Nicolson scheme [44].

The rest of the paper is organized as follows. In Sects. 2 and 3, we discuss the model and its one-dimensional version together with stability results. Here we present, for the first time, a proof of the energy relation of the nonlinear Maxwell model that was presented in our prior work [5]. Sections 4–6 present the semi-discrete and fully discrete numerical methods.

Section 7 considers the generalization to nonuniform grids for $M = 1$. Section 8 contains the numerical results, and some technical details are collected in the ‘‘Appendix’’.

2 Maxwell’s Equations and Constitutive Laws for Nonlinear Optical Materials

We use the auxiliary differential equation (ADE) approach, and append to Maxwell’s partial differential equations (PDEs) a system of ODEs describing the nonlinear relationship between the macroscopic polarization vector \mathbf{P} and the electric field \mathbf{E} . Our approach follows the development in [16]. The hybrid system of Maxwell PDEs and auxiliary ODEs are then simultaneously evolved in time. Below we discuss a *polarization* model that incorporates an instantaneous nonlinear Kerr effect as well as both linear and nonlinear dispersive effects, the latter described as Raman scattering.

Let $T > 0$. We begin by introducing Maxwell’s equations in a non-magnetic, non-conductive medium $\Omega \subset \mathbb{R}^d$, $d = 1, 2, 3$, containing no free charges, that govern the dynamic evolution of the electric field \mathbf{E} and the magnetic field \mathbf{H} in the form

$$\partial_t \mathbf{B} + \nabla \times \mathbf{E} = 0, \text{ in } (0, T) \times \Omega, \tag{2.1a}$$

$$\partial_t \mathbf{D} - \nabla \times \mathbf{H} = 0, \text{ in } (0, T) \times \Omega, \tag{2.1b}$$

$$\nabla \cdot \mathbf{B} = 0, \nabla \cdot \mathbf{D} = 0, \text{ in } (0, T) \times \Omega, \tag{2.1c}$$

along with initial and boundary data. System (2.1) has to be completed by constitutive laws on $[0, T] \times \Omega$. The electric flux density \mathbf{D} , and the magnetic induction \mathbf{B} , are related to the electric field and magnetic field, respectively, via the constitutive laws

$$\mathbf{D} = \epsilon_0(\epsilon_\infty \mathbf{E} + \mathbf{P}), \quad \mathbf{B} = \mu_0 \mathbf{H}. \tag{2.2}$$

The parameter ϵ_0 is the electric permittivity of free space, while μ_0 is the magnetic permeability of free space. The term $\epsilon_\infty \mathbf{E}$ captures the linear instantaneous response of the material to the EM fields, with ϵ_∞ defined as the relative electric permittivity in the limit of infinite frequencies. The macroscopic (*electric*) *polarization* \mathbf{P} includes both linear and nonlinear effects, and is related to the electric field via the constitutive law

$$\mathbf{P} = \underbrace{\mathbf{P}_{\text{delay}}^{\text{L}}}_{\text{linear}} + \underbrace{a(1 - \theta)\mathbf{E}|\mathbf{E}|^2}_{\text{Kerr}} + \underbrace{a\theta \mathbf{Q}\mathbf{E}}_{\text{Raman}}. \tag{2.3}$$

In (2.3), we model the linear retarded response $\mathbf{P}_{\text{delay}}^{\text{L}}$ as a single resonance Lorentz dispersion model coupled to the electric field intensity \mathbf{E} . The time dependent evolution of $\mathbf{P}_{\text{delay}}^{\text{L}}$ follows the second order ODE [16,44]

$$\frac{\partial^2 \mathbf{P}_{\text{delay}}^{\text{L}}}{\partial t^2} + \frac{1}{\tau} \frac{\partial \mathbf{P}_{\text{delay}}^{\text{L}}}{\partial t} + \omega_0^2 \mathbf{P}_{\text{delay}}^{\text{L}} = \omega_p^2 \mathbf{E}. \tag{2.4}$$

In the ODE (2.4), ω_0 and ω_p are the resonance and plasma frequencies of the medium, respectively, and τ^{-1} is a damping constant. The plasma frequency is related to the resonance frequency via the relation $\omega_p^2 = (\epsilon_s - \epsilon_\infty)\omega_0^2 := \epsilon_d \omega_0^2$. Here ϵ_s is defined as the relative permittivity at zero frequency, and ϵ_d measures the strength of the electric field coupling to the linear Lorentz dispersion model. We note that the limit $\epsilon_d \rightarrow 0$, or $\epsilon_s \rightarrow \epsilon_\infty$ corresponds to the linear dispersionless situation.

To observe nonlinear effects in common materials, high-intensity light sources, such as lasers, are required, and the particular nonlinear effects observed depend on which term is dominant in the electric polarization [25]. We will consider materials in which the dominant nonlinearities are of the third order (such as optical glass fibers) and include instantaneous as well as delayed material responses. In particular, in (2.3) we consider a cubic instantaneous response modeled by the electronic Kerr effect, which is a phenomenon in which the refractive index of a material changes proportionally to the square of the applied electric field. The nonlinear retarded effect (Raman) in (2.3) is a molecular vibrational response called Raman scattering. It is captured by the variable Q which describes the natural molecular vibrations within the dielectric material responding to the nonlinear electric field intensity at frequencies much smaller than the optical wave frequency [17]. Like the linear Lorentz dispersion model for the linear retarded response, the nonlinear retarded response Q is also modeled by a single resonance Lorentz dispersion model, but coupled to the nonlinear field intensity $|\mathbf{E}|^2$. The dynamic evolution of Q follows the second order nonlinear ODE

$$\frac{\partial^2 Q}{\partial t^2} + \frac{1}{\tau_v} \frac{\partial Q}{\partial t} + \omega_v^2 Q = \omega_v^2 |\mathbf{E}|^2, \tag{2.5}$$

where ω_v is the resonance frequency of the vibration, and τ_v^{-1} is a damping constant. In order to arrive at the ODE for Q , we have assumed an axially symmetric and isotropic environment. The parameter a in (2.3) is a third order coupling constant, while θ parameterizes the relative strength of the instantaneous Kerr response and retarded Raman molecular vibrational responses. In the limit $\theta \rightarrow 0$, the nonlinear response reduces to the instantaneous intensity-dependent Kerr response.

Taking all effects into account, the constitutive laws for \mathbf{D} and \mathbf{B} can be rewritten as

$$\mathbf{D} = \epsilon_0(\epsilon_\infty \mathbf{E} + \mathbf{P}_{\text{delay}}^L + a(1 - \theta)\mathbf{E}|\mathbf{E}|^2 + a\theta Q\mathbf{E}), \quad \mathbf{B} = \mu_0 H. \tag{2.6}$$

With this, the mathematical model for EM wave propagation in the nonlinear optical medium is the hybrid system (2.1), (2.4), (2.5) and (2.6).

3 Nonlinear Maxwell’s Equations in 1D: Model and Energy Relations

In this paper, we focus on a one dimensional nonlinear Maxwell model that is obtained from (2.1), (2.4), (2.5) and (2.6) by assuming an isotropic and homogeneous material in which electromagnetic plane waves are linearly polarized and propagate in the x direction. Thus, the electric field is represented by one scalar component $E := E_z$, while the magnetic field is represented by the one component $H := H_y$. All the other variables are similarly represented by single scalar components. We convert the second order ODE (2.4) for the retarded linear polarization $P := P_{\text{delay}}^L$, and the ODE (2.5) for molecular vibrations Q , to first order form by introducing the linear polarization density J , and the nonlinear conductivity σ , respectively.

Let $\Omega \subset \mathbb{R}$. The one spatial dimensional nonlinear Maxwell system on $(0, T) \times \Omega$ is

$$\mu_0 \frac{\partial H}{\partial t} = \frac{\partial E}{\partial x}, \tag{3.1a}$$

$$\frac{\partial D}{\partial t} = \frac{\partial H}{\partial x}, \tag{3.1b}$$

$$\frac{\partial P}{\partial t} = J, \tag{3.1c}$$

$$\frac{\partial J}{\partial t} = -\frac{1}{\tau}J - \omega_0^2 P + \omega_p^2 E, \tag{3.1d}$$

$$\frac{\partial Q}{\partial t} = \sigma, \tag{3.1e}$$

$$\frac{\partial \sigma}{\partial t} = -\frac{1}{\tau_v}\sigma - \omega_v^2 Q + \omega_v^2 E^2, \tag{3.1f}$$

along with the constitutive law

$$D = \epsilon_0(\epsilon_\infty E + P + a(1 - \theta)E^3 + a\theta QE), \tag{3.2}$$

and appropriate initial and boundary data. We note that Gauss’s laws (2.1c) for this one dimensional case only involve the x derivatives of the first components of \mathbf{B} and \mathbf{D} . These components are decoupled from the one-dimensional model (3.1) and become irrelevant for the case considered here.

We now state and prove an energy result that establishes the stability of the solution to the one dimensional nonlinear Maxwell’s equations (3.1)–(3.2), when the solutions satisfy periodic boundary conditions on Ω . This energy relation was first presented in our previous work [5], and a discrete analog of the energy relation for DG methods was also established. Here we present for the first time, the proof of this energy result.

Theorem 3.1 *Let $\theta \in [0, \frac{3}{4}]$. Assuming periodic boundary conditions for all fields on Ω , the nonlinear Maxwell system (3.1)–(3.2) satisfies the energy identity:*

$$\frac{d}{dt} \mathcal{E}_\theta(t) = - \int_\Omega \left(\frac{\epsilon_0}{\tau \omega_p^2} J^2 + \frac{a\theta \epsilon_0}{2\tau_v \omega_v^2} \sigma^2 \right) dx, \tag{3.3}$$

where

$$\begin{aligned} \mathcal{E}_\theta(t) := & \frac{1}{2} \int_\Omega \left(\mu_0 H^2 + \epsilon_0 \epsilon_\infty E^2 + \frac{\epsilon_0}{\epsilon_d} P^2 + \frac{\epsilon_0}{\omega_p^2} J^2 + \frac{a\theta \epsilon_0}{2\omega_v^2} \sigma^2 \right. \\ & \left. + \frac{a\theta \epsilon_0}{2} (Q + E^2)^2 + \frac{a\epsilon_0}{2} (3 - 4\theta) E^4 \right) dx. \end{aligned} \tag{3.4}$$

The function $\mathcal{E}_\theta(t) \geq 0$ for the chosen range of the parameter θ .

Proof Substituting Eq. (3.2) in Eq. (3.1b), we get

$$\frac{\partial}{\partial t} (\epsilon_0(\epsilon_\infty E + a(1 - \theta)E^3 + P + a\theta QE)) = \frac{\partial H}{\partial x}. \tag{3.5}$$

Multiplying Eq. (3.1a) by H , Eq. (3.5) by E , Eq. (3.1c) by $\frac{\epsilon_0}{\epsilon_d} P$, Eq. (3.1d) by $\frac{\epsilon_0}{\omega_p^2} J$, Eq. (3.1e) by $a\theta \epsilon_0 Q$ and the Eq. (3.1f) by $\frac{a\theta \epsilon_0}{\omega_v^2} \sigma$, and then summing over all equations and using Eq. (3.1c) we obtain

$$\begin{aligned} & \frac{1}{2} \frac{\partial}{\partial t} \left[\mu_0 H^2 + \epsilon_0 \epsilon_\infty E^2 + \frac{\epsilon_0}{\epsilon_d} P^2 + \frac{\epsilon_0}{\omega_p^2} J^2 + a\theta \epsilon_0 Q^2 + \frac{a\theta \epsilon_0}{\omega_v^2} \sigma^2 \right] + a\epsilon_0(1 - \theta)E \frac{\partial E^3}{\partial t} \\ & + a\theta \epsilon_0 E \frac{\partial}{\partial t} (QE) - a\theta \epsilon_0 \sigma E^2 = H \frac{\partial E}{\partial x} + E \frac{\partial H}{\partial x} - \frac{\epsilon_0}{\tau \omega_p^2} J^2 - \frac{a\theta \epsilon_0}{\tau_v \omega_v^2} \sigma^2. \end{aligned} \tag{3.6}$$

We can rewrite the nonlinear term in E^3 on the left hand side in Eq. (3.6) as

$$a\epsilon_0(1 - \theta)E \frac{\partial E^3}{\partial t} = a\epsilon_0(1 - \theta)(3E^3) \frac{\partial E}{\partial t} = \frac{3}{2}a\epsilon_0(1 - \theta) \frac{\partial}{\partial t} \left(\frac{E^4}{2} \right). \tag{3.7}$$

Using Eq. (3.1e), we simplify the last two nonlinear terms on the left hand side in Eq. (3.6) as

$$a\theta\epsilon_0E \frac{\partial}{\partial t}(QE) - a\theta\epsilon_0\sigma E^2 = a\theta\epsilon_0Q \frac{\partial}{\partial t} \left(\frac{E^2}{2} \right) = a\theta\epsilon_0 \frac{\partial}{\partial t} \left(\frac{QE^2}{2} \right) - \frac{a\theta\epsilon_0}{2} \sigma E^2. \tag{3.8}$$

To obtain a bound on the last term in (3.8), we multiply Eq. (3.1f) by $\frac{a\theta\epsilon_0}{2\omega_v^2}\sigma$, and then using Eq. (3.1e), we obtain

$$\frac{a\theta\epsilon_0}{2} \sigma E^2 = \frac{a\theta\epsilon_0}{2\omega_v^2} \frac{\partial}{\partial t} \left(\frac{\sigma^2}{2} \right) + \frac{a\theta\epsilon_0}{2\omega_v^2\tau_v} \sigma^2 + \frac{a\theta\epsilon_0}{2} \frac{\partial}{\partial t} \left(\frac{Q^2}{2} \right). \tag{3.9}$$

Next we combine Eqs. (3.6)–(3.9) and simplify to get the identity

$$\begin{aligned} & \frac{1}{2} \frac{\partial}{\partial t} \left[\mu_0 H^2 + \epsilon_0 \epsilon_\infty E^2 + \frac{\epsilon_0}{\epsilon_d} P^2 + \frac{\epsilon_0}{\omega_p^2} J^2 \right. \\ & \quad \left. + \frac{a\theta\epsilon_0}{2\omega_v^2} \sigma^2 + \frac{a\theta\epsilon_0}{2} Q^2 + \frac{3}{2} a\epsilon_0(1 - \theta) E^4 + a\theta\epsilon_0 Q E^2 \right] \\ & = H \frac{\partial E}{\partial x} + E \frac{\partial H}{\partial x} - \frac{\epsilon_0}{\tau \omega_p^2} J^2 - \frac{a\theta\epsilon_0}{2\tau_v \omega_v^2} \sigma^2. \end{aligned} \tag{3.10}$$

The last three terms on the left hand side in (3.10) can be rewritten in the form

$$\frac{a\theta\epsilon_0}{2} Q^2 + \frac{3}{2} a\epsilon_0(1 - \theta) E^4 + a\theta\epsilon_0 Q E^2 = \frac{a\theta\epsilon_0}{2} (Q + E^2)^2 + \frac{a\epsilon_0}{2} (3 - 4\theta) E^4. \tag{3.11}$$

From (3.10) and (3.11), we obtain the identity

$$\begin{aligned} & \frac{1}{2} \frac{\partial}{\partial t} \left[\mu_0 H^2 + \epsilon_0 \epsilon_\infty E^2 + \frac{\epsilon_0}{\epsilon_d} P^2 + \frac{\epsilon_0}{\omega_p^2} J^2 \right. \\ & \quad \left. + \frac{a\theta\epsilon_0}{2\omega_v^2} \sigma^2 + \frac{a\theta\epsilon_0}{2} (Q + E^2)^2 + \frac{a\epsilon_0}{2} (3 - 4\theta) E^4 \right] \\ & = H \frac{\partial E}{\partial x} + E \frac{\partial H}{\partial x} - \frac{\epsilon_0}{\tau \omega_p^2} J^2 - \frac{a\theta\epsilon_0}{2\tau_v \omega_v^2} \sigma^2. \end{aligned} \tag{3.12}$$

Integrating (3.12) over the domain Ω , integrating by parts in the first two terms on the right hand side, using the periodic boundary conditions, and the definition of the energy $\mathcal{E}_\theta(t)$ in (3.4), we obtain the energy identity

$$\frac{1}{2} \frac{d}{dt} \mathcal{E}_\theta(t) = - \int_\Omega \left(\frac{\epsilon_0}{\tau \omega_p^2} J^2 + \frac{a\theta\epsilon_0}{2\tau_v \omega_v^2} \sigma^2 \right) dx,$$

which is Eq. (3.3) in the theorem. □

4 Construction of High Order Spatial Approximations

In this section we describe the construction of high order approximations to the first order derivative operator $\partial/\partial x$. The construction presented in this section follows the exposition in [2,4,8].

Let $L > 0, L \in \mathbb{R}$. Following the notation in [8, p. 36], we introduce staggered ℓ^2 normed spaces with periodic boundary conditions. Consider smooth functions v and u defined on \mathbb{R} satisfying periodic conditions $v(x) = v(x + L)$ and $u(x) = u(x + L), \forall x \in \mathbb{R}$.

Based on the periodicity, we focus on constructing numerical methods on the computational domain $\Omega = [0, L]$. Let $\Delta x = h = L/I > 0$, for some positive integer I , be a uniform mesh step size. Define $x_j = jh, 0 \leq j \leq I$ and $x_{j+\frac{1}{2}} = (j + \frac{1}{2})h, 0 \leq j \leq I - 1$. We define two staggered grids on Ω . The *primal grid*, G_p , is defined as

$$G_p : x_0 < x_1 < x_2 < \dots < x_{I-1} < x_I. \tag{4.1}$$

The *dual grid*, G_d , on $[0, L]$ is defined as

$$G_d : x_{\frac{1}{2}} < x_{\frac{3}{2}} < x_{\frac{5}{2}} < \dots < x_{I-\frac{1}{2}}. \tag{4.2}$$

Define $v_\ell \approx v(x_\ell)$ and $u_{\ell+\frac{1}{2}} \approx u(x_{\ell+\frac{1}{2}})$. On the primal grid G_p we define the discrete space

$$V_{0,h} := \{v_h := (v_\ell), 0 \leq \ell \leq I - 1, v_0 = v_I \mid h \sum_{\ell=0}^{I-1} |v_\ell|^2 < \infty\}, \tag{4.3}$$

and on the dual grid G_d , we define the discrete space

$$V_{\frac{1}{2},h} := \left\{ u_h := \left(u_{\ell+\frac{1}{2}} \right), 0 \leq \ell \leq I - 1, u_{\frac{1}{2}} = u_{I+\frac{1}{2}} \mid h \sum_{\ell=0}^{I-1} |u_{\ell+\frac{1}{2}}|^2 < \infty \right\}. \tag{4.4}$$

The ℓ^2 norms on $V_{0,h}$, and $V_{\frac{1}{2},h}$, denoted by $\|\cdot\|_{0,h}$, and $\|\cdot\|_{\frac{1}{2},h}$, respectively, are defined as

$$\|v_h\|_{0,h} := \left(h \sum_{\ell=0}^{I-1} |v_\ell|^2 \right)^{1/2}, \forall v_h \in V_{0,h}, \tag{4.5}$$

$$\|u_h\|_{\frac{1}{2},h} := \left(h \sum_{\ell=0}^{I-1} |u_{\ell+\frac{1}{2}}|^2 \right)^{1/2}, \forall u_h \in V_{\frac{1}{2},h}, \tag{4.6}$$

derived from corresponding ℓ^2 scalar products $\langle \cdot, \cdot \rangle_{0,h}$, and $\langle \cdot, \cdot \rangle_{\frac{1}{2},h}$.

Next, we outline the construction of high order discrete approximations of $\partial/\partial x$. For $p \in \mathbb{N}$, we define the discrete finite difference operators

$$\mathcal{D}_{p,h}^{(2)} : V_{0,h} \rightarrow V_{\frac{1}{2},h}, \left(\mathcal{D}_{p,h}^{(2)} v_h \right)_{\ell+\frac{1}{2}} := \frac{v_{\ell+p} - v_{\ell-p+1}}{(2p-1)h}, \forall v_h \in V_{0,h}, \tag{4.7a}$$

$$\tilde{\mathcal{D}}_{p,h}^{(2)} : V_{\frac{1}{2},h} \rightarrow V_{0,h}, \left(\tilde{\mathcal{D}}_{p,h}^{(2)} u_h \right)_\ell := \frac{u_{\ell+p-\frac{1}{2}} - u_{\ell-p+\frac{1}{2}}}{(2p-1)h}, \forall u_h \in V_{\frac{1}{2},h}. \tag{4.7b}$$

These are second-order discrete approximations of the operator $\partial/\partial x$ computed with stepsize $(2p - 1)h$. If we let \mathcal{D}^* to be the adjoint of the discrete operator \mathcal{D} with respect to the ℓ^2 scalar product, then $\tilde{\mathcal{D}}_{p,h}^{(2)} = -\left(\mathcal{D}_{p,h}^{(2)} \right)^*$.

Following the work done in [2] (see ‘‘Appendix A’’ for some details), we construct finite difference approximations of order $2M$, $M \in \mathbb{N}$, of the first order operator $\partial/\partial x$, by taking linear combinations of second order approximations (4.7) to $\partial/\partial x$ computed with different space steps $(2p - 1)h$ and choosing the coefficients in the linear combination to obtain $2M$ order accuracy. Thus, we have the operator definitions

$$\mathcal{D}_h^{(2M)} : V_{0,h} \rightarrow V_{\frac{1}{2},h}, \mathcal{D}_h^{(2M)} := \sum_{p=1}^M \lambda_{2p-1}^{2M} \mathcal{D}_{p,h}^{(2)}, \tag{4.8a}$$

$$\tilde{\mathcal{D}}_h^{(2M)} : V_{\frac{1}{2},h} \rightarrow V_{0,h}, \tilde{\mathcal{D}}_h^{(2M)} := \sum_{p=1}^M \lambda_{2p-1}^{2M} \tilde{\mathcal{D}}_{p,h}^{(2)}. \tag{4.8b}$$

Similar to the case of second order operators, if we let $(\mathcal{D}_h^{(2M)})^*$ to be the adjoint of the discrete operator $\mathcal{D}_h^{(2M)}$ with respect to the $V_{0,h}$ scalar product, then we have $\tilde{\mathcal{D}}_h^{(2M)} = -(\mathcal{D}_h^{(2M)})^*$. It can be shown that (see [8, p. 53] and [6]), in order to obtain discrete approximations to $\partial/\partial x$ with at least $2M$ order accuracy, the coefficients λ_{2p-1}^{2M} in (4.8) have to be chosen according to an explicit formula given in the theorem below. To state this formula we need the definition of the the double factorial. For $1 \leq n \leq M$, the double factorial $n!!$ is defined as

$$n!! = \begin{cases} n \cdot (n - 2) \cdot (n - 4) \dots 5 \cdot 3 \cdot 1 & n > 0, \text{ odd} \\ n \cdot (n - 2) \cdot (n - 4) \dots 6 \cdot 4 \cdot 2 & n > 0, \text{ even} \\ 1, & n = -1, 0. \end{cases} \tag{4.9}$$

Theorem 4.1 *For any $M \in \mathbb{N}$ and for sufficiently smooth functions, a necessary and sufficient condition for the discrete difference operators in (4.8), as finite difference approximations of the continuous differential operator $\partial/\partial x$, to provide at least $2M$ order of accuracy, is given by the explicit formula*

$$\lambda_{2p-1}^{2M} = \frac{2(-1)^{p-1}[(2M - 1)!!]^2}{(2M + 2p - 2)!!(2M - 2p)!!(2p - 1)}, \forall p, 1 \leq p \leq M, \tag{4.10}$$

for the coefficients λ_{2p-1}^{2M} in the linear combinations in the definition of the operators (4.8).

Proof See ‘‘Appendix’’. □

5 Fully Discrete Leap-Frog FDTD Methods

In this section, we derive fully discrete FDTD methods on $[0, T] \times \Omega$, using the high order spatial discretizations outlined in Sect. 4, and second order temporal discretizations based on the leap-frog time integrator. Our methods will have second order accuracy in time and $2M$ -th order accuracy in space, $M \in \mathbb{N}$. We will call these schemes $(2, 2M)$ leap-frog FDTD methods.

Let $N > 0$ be a positive integer. Define $\Delta t > 0$ such that $N\Delta t = T$. Analogous to the uniform spatial discretization on $[0, L]$, we also define primal and dual temporal meshes using time points $t^n = n\Delta t$, for $n = 0, 1, 2, \dots, N$, with $t^N = T$, and $t^{n+\frac{1}{2}} = (n + \frac{1}{2})\Delta t$, for $n = 0, 1, 2, \dots, N - 1$. The discrete magnetic field will be computed at dual spatial

and temporal nodes, while all the other discrete fields will be computed at primal spatial and temporal nodes in the space–time mesh. For a field variable $V(t, x)$, we denote the approximation of $V(t^n, x_j)$ by V_j^n on the primal space–time mesh and the approximation of $V(t^{n+\frac{1}{2}}, x_{j+\frac{1}{2}})$ by $V_{j+\frac{1}{2}}^{n+\frac{1}{2}}$ on the dual space–time mesh. We assume the periodic boundary conditions $V_0^n = V_I^n$ for $n = 0, 1, \dots, N$, on the primal space–time mesh, while on the dual space–time mesh we assume $V_{\frac{1}{2}}^{n+\frac{1}{2}} = V_{I+\frac{1}{2}}^{n+\frac{1}{2}}, \forall n = 0, 1, 2, \dots, N - 1$. Thus, the magnetic field is staggered in space–time from all the other field variables.

We discretize the system (3.1a)–(3.1f) using the high order $2M, M \in \mathbb{N}$ spatial discretizations defined in Sect. 4, and a modified second order leap-frog scheme in time on the dual space–time mesh for the magnetic field and the primal space–time mesh for all the other field variables. Our fully discrete $(2, 2M)$ leap-frog FDTD schemes for the discretization of the nonlinear Maxwell problem (3.1)–(3.2) are given as below.

Assume $D_h^0, E_h^0, P_h^0, J_h^0, Q_h^0, \sigma_h^0, Y_h^0 \in V_{0,h}$ and $H_h^{-\frac{1}{2}} \in V_{\frac{1}{2},h}$ are given. Then $\forall n \in \mathbb{N}$, with $0 < n \leq N$, find $D_h^n, E_h^n, P_h^n, J_h^n, Q_h^n, \sigma_h^n, Y_h^n \in V_{0,h}$ and $H_h^{n+\frac{1}{2}} \in V_{\frac{1}{2},h}$ satisfying, $\forall j$ with $0 \leq j \leq I$, the system of equations $\forall 0 \leq j \leq I$,

$$\mu_0 \frac{H_{j+\frac{1}{2}}^{n+\frac{1}{2}} - H_{j+\frac{1}{2}}^{n-\frac{1}{2}}}{\Delta t} = \left(\mathcal{D}_h^{(2M)} E_h^n \right)_{j+\frac{1}{2}}, \tag{5.1a}$$

$$\frac{D_j^{n+1} - D_j^n}{\Delta t} = \left(\tilde{\mathcal{D}}_h^{(2M)} H_h^{n+\frac{1}{2}} \right)_j, \tag{5.1b}$$

$$\frac{P_j^{n+1} - P_j^n}{\Delta t} = \frac{1}{2} \left(J_j^{n+1} + J_j^n \right), \tag{5.1c}$$

$$\frac{J_j^{n+1} - J_j^n}{\Delta t} = -\frac{1}{2\tau} \left(J_j^{n+1} + J_j^n \right) - \frac{\omega_0^2}{2} \left(P_j^{n+1} + P_j^n \right) + \frac{\omega_p^2}{2} \left(E_j^{n+1} + E_j^n \right), \tag{5.1d}$$

$$\frac{Q_j^{n+1} - Q_j^n}{\Delta t} = \frac{1}{2} \left(\sigma_j^{n+1} + \sigma_j^n \right), \tag{5.1e}$$

$$\frac{\sigma_j^{n+1} - \sigma_j^n}{\Delta t} = -\frac{1}{2\tau_v} \left(\sigma_j^{n+1} + \sigma_j^n \right) - \frac{\omega_v^2}{2} \left(Q_j^{n+1} + Q_j^n \right) + \omega_v^2 E_j^n E_j^{n+1}, \tag{5.1f}$$

$$D_j^{n+1} = \epsilon_0 \left(\epsilon_\infty E_j^{n+1} + P_j^{n+1} + a(1 - \theta) Y_j^{n+1} + a\theta Q_j^{n+1} E_j^{n+1} \right), \tag{5.1g}$$

with

$$Y_j^{n+1} = Y_j^n + \frac{3}{2} \left((E_j^{n+1})^2 + (E_j^n)^2 \right) \left(E_j^{n+1} - E_j^n \right). \tag{5.2}$$

There are three nonlinear terms whose discretization is crucial to building energy stable fully discrete numerical methods. The nonlinear term E^2 is discretized on the primal space–time mesh as the product $E_j^n E_j^{n+1}$ in Eq. (5.1f). In [16], this term is discretized as an average of E_j^n and E_j^{n+1} . We do not know if this latter discretization leads to a fully discrete energy stable method. The second nonlinearity QE is discretized on the primal space–time mesh as $Q_j^n E_j^n$ as seen in Eq. (5.1g). Lastly, the grid function Y_h^n in Eq. (5.2) is a discrete approximation of the continuous cubic power E^3 . The introduction of Y_h^n is a novelty of the modified leap-frog scheme that allows us to correctly (in the sense of energy conservation) discretize E^3 on the

discrete mesh, since if $Y = E^3$, then $dY = 3E^2dE$, which is precisely what Eq. (5.2) is simulating. While we do introduce a new variable, we note that we do not need to explicitly store $Y_h^n, \forall n$ in our actual implementations. Only the difference in $Y_h^{n+1} - Y_h^n$ needs to be stored.

We will now prove that for fixed $M \in \mathbb{N}$, the $(2, 2M)$ leap-frog FDTD scheme (5.1)–(5.2) satisfies a discrete energy decay identity consistent with Theorem 3.1, under appropriate Courant–Friedrich–Lewy (CFL) conditions that depend on the value of M . We first state the following identity that is a discrete analogue of integration by parts, and is called a *summation by parts* identity.

Lemma 5.1 *Consider the grid functions $U_h \in V_{0,h}$ and $W_h \in V_{\frac{1}{2},h}$. Then, the following summation by parts identity holds*

$$\sum_{j=0}^{I-1} \left(\mathcal{D}_h^{(2M)} U_h \right)_{j+\frac{1}{2}} W_{j+\frac{1}{2}} = - \sum_{j=0}^{I-1} \left(\tilde{\mathcal{D}}_h^{(2M)} W_h \right)_j U_j, \tag{5.3}$$

Some details of similar proofs can be found in [8].

Next, we prove the positive definiteness of an operator, which is an important ingredient in the proof of stability of the fully discrete leap-frog FDTD method.

Theorem 5.2 *Consider the operator $\mathcal{A}_h : V_{0,h} \rightarrow V_{0,h}$ defined as*

$$\mathcal{A}_h := I_h + \gamma^2 \tilde{\mathcal{D}}_h^{(2M)} \circ \mathcal{D}_h^{(2M)}, \tag{5.4}$$

where $I_h : V_{0,h} \rightarrow V_{0,h}$ is the identity operator, the $2M, M \in \mathbb{N}$ order spatial discretizations are as defined in (4.8), and $\gamma = \frac{c_\infty \Delta t}{2}$ is a constant independent of the mesh step h , but depends on Δt and the speed $c_\infty := \sqrt{\frac{1}{\epsilon_0 \epsilon_\infty \mu_0}}$. The operator \mathcal{A}_h is positive definite if and only if γ satisfies the condition

$$\frac{2\gamma}{h} < \frac{1}{\sum_{\ell=1}^M \frac{[(2\ell - 3)!!]^2}{(2\ell - 1)!}}. \tag{5.5}$$

Proof For $M \in \mathbb{N}$, the operator $\mathcal{A}_{1,h}^{(2M)} : V_{0,h} \rightarrow V_{0,h}$ defined as

$$\mathcal{A}_{1,h}^{(2M)} := \tilde{\mathcal{D}}_h^{(2M)} \circ \mathcal{D}_h^{(2M)}, \tag{5.6}$$

is a $2M$ -th order approximation of the 1D Laplacian $\frac{\partial^2}{\partial x^2}$ [8]. The condition for positivity of operator \mathcal{A}_h in (5.4) is obtained by analyzing the symbol of operator $\mathcal{A}_{1,h}^{(2M)}$, which is computed by using the discrete Fourier transform (DFT), defined as

$$\mathcal{F}_h : V_{0,h} \rightarrow \ell^2 \left(\left[\frac{-\pi}{h}, \frac{\pi}{h} \right] \right) \tag{5.7}$$

$$\mathcal{F}_h(u_h)(k) = \frac{h}{\sqrt{2\pi}} \sum_{j=0}^{I-1} u_j e^{-ikx_j}, \quad \forall u_h \in V_{0,h}, \forall k \in \left[\frac{-\pi}{h}, \frac{\pi}{h} \right]. \tag{5.8}$$

where the mesh step size $h = L/I$, for positive I . We will assume below that I is even. Also, $k \in \left[-\frac{\pi}{h}, \frac{\pi}{h} \right]$ is a discrete wave number defined as $k = \frac{2\pi m}{L}$, with m an integer, taking values in $\left[-\frac{I}{2}, \frac{I}{2} \right]$. The reason for choosing a bounded, and discrete domain for wave numbers k is

due to aliasing occurring when the spatial variable x is discrete, and due to a bounded spatial domain, respectively. The choice of $|m| \leq \frac{L}{2}$ is due to the Nyquist limit which requires a resolution of at least two points per wavelength. For example, the choice $m = \frac{L}{2}$ gives a wave number $k = \frac{\pi L}{L}$, which corresponds to a wavelength of $\lambda := \frac{2\pi}{k} = \frac{2L}{L} = 2h$.

The space $L^2\left(\left[-\frac{\pi}{h}, \frac{\pi}{h}\right]\right)$ denotes the space of L periodic functions of k on the grid \mathbb{Z} with norm

$$\|\mathcal{F}_h(u_h)\|_{L^2\left(\left[-\frac{\pi}{h}, \frac{\pi}{h}\right]\right)} = \left(\sum_{k=-\pi/h}^{\pi/h} |\mathcal{F}_h(u_h)(k)|^2 \right)^{1/2}, \quad \forall u_h \in V_{0,h}, \tag{5.9}$$

Using the results in [8] it can be shown that the Fourier transform of $\mathcal{A}_h u_h$ is

$$\mathcal{F}_h(\mathcal{A}_h u_h)(k) = (\mathcal{S}_h(\mathcal{A}_h)(k)) (\mathcal{F}_h(u_h)(k)), \quad \forall k \in \left[-\frac{\pi}{h}, \frac{\pi}{h}\right], \tag{5.10}$$

where $\mathcal{S}_h(\mathcal{A}_h)$ is the symbol of the operator \mathcal{A}_h , and is computed to be

$$\mathcal{S}_h(\mathcal{A}_h)(k) = \left(1 - \frac{4\gamma^2}{h^2} \left[\sum_{p=1}^M \frac{\lambda_{2p-1}^{(2M)}}{2p-1} \sin\left((2p-1)\frac{kh}{2}\right) \right]^2 \right), \quad \forall k \in \left[-\frac{\pi}{h}, \frac{\pi}{h}\right]. \tag{5.11}$$

from the symbol, $\mathcal{S}_h(\mathcal{A}_{1,h}^{2M})$ of the operator $\mathcal{A}_{1,h}^{2M}$ given as

$$\mathcal{S}_h(\mathcal{A}_{1,h}^{2M})(k) = -\frac{4}{h^2} \sum_{p=1}^M \frac{\lambda_{2p-1}^{(2M)}}{2p-1} \left[\sin\left((2p-1)\frac{kh}{2}\right) \right]^2, \quad \forall k \in \left[-\frac{\pi}{h}, \frac{\pi}{h}\right]. \tag{5.12}$$

Using the results in [4,8], this symbol can be rewritten as (see ‘‘Appendix B’’ for details)

$$\mathcal{S}_h(\mathcal{A}_h)(k) = \left(1 - \frac{4\gamma^2}{h^2} \left[\sum_{p=1}^M \frac{[(2p-3)!!]^2}{(2p-1)!} \sin^{2p-1}\left(\frac{kh}{2}\right) \right]^2 \right), \quad \forall k \in \left[-\frac{\pi}{h}, \frac{\pi}{h}\right]. \tag{5.13}$$

The operator \mathcal{A}_h is bounded and positive if its symbol $\mathcal{S}_h(\mathcal{A}_h)$ is bounded and positive for all wave numbers k such that $|kh| \leq \pi$ ([8]). As shown in [4], all of the coefficients of the sine terms in the symbol (5.13) are strictly positive. Thus, for $\mathcal{S}_h(\mathcal{A}_h)$ to be positive we must have

$$\frac{2\gamma}{h} < \left[\sup_{|kh| \leq \pi} \left(\sum_{\ell=1}^M \frac{[(2\ell-3)!!]^2}{(2\ell-1)!} \sin^{2\ell-1}\left(\frac{kh}{2}\right) \right) \right]^{-1}. \tag{5.14}$$

The supremum in the right hand side of inequality (5.14) is attained at $kh = \pi$, or when $m = \frac{L}{2}$, from which we get the condition for positivity of the symbol $\mathcal{S}_h(\mathcal{A}_h)$ and thus for the positivity of the operator \mathcal{A}_h to be

$$\frac{2\gamma}{h} < \left[\sum_{\ell=1}^M \frac{[(2\ell-3)!!]^2}{(2\ell-1)!} \right]^{-1}. \tag{5.15}$$

□

Consider a discrete grid function $V_h^n \in V_{0,h}$ for $n = 0, 1, \dots, N$. We define $\overline{V}_h^{n+\frac{1}{2}}$ to be the average of V_h^n and V_h^{n+1} , i.e. on $V_{0,h}$, we have

$$\overline{V}_h^{n+\frac{1}{2}} := \frac{1}{2} \left(V_h^n + V_h^{n+1} \right). \tag{5.16}$$

We similarly define the grid function $\overline{V}_h^n \in V_{\frac{1}{2},h}$ to be the average of $V_h^{n+\frac{1}{2}}$ and $V_h^{n-\frac{1}{2}}$ in $V_{\frac{1}{2},h}$, i.e.,

$$\overline{V}_h^n := \frac{1}{2} \left(V_h^{n+\frac{1}{2}} + V_h^{n-\frac{1}{2}} \right). \tag{5.17}$$

Next, we prove our main stability result for the modified leap-frog schemes. The $(2, 2M)$ order leap-frog schemes satisfy the following energy identity.

Theorem 5.3 *Let $0 \leq n \leq N$. Let $H_h^{n+\frac{1}{2}} \in V_{\frac{1}{2},h}$, $E_h^n, P_h^n, J_h^n, \sigma_h^n, Q_h^n \in V_{0,h}$, and assume $\theta \in [0, \frac{3}{4}]$. Under the CFL condition*

$$\frac{c_\infty \Delta t}{h} < \left[\sum_{\ell=1}^M \frac{[(2\ell - 3)!!]^2}{(2\ell - 1)!} \right]^{-1}, \tag{5.18}$$

the $(2, 2M)$ order leap-frog FDTD scheme (5.1) satisfies the discrete energy identity

$$\frac{\mathcal{E}_{h,\text{LF}}^{n+1} - \mathcal{E}_{h,\text{LF}}^n}{\Delta t} = -\frac{\epsilon_0}{\tau \omega_p^2} \|\overline{J}_h^{n+\frac{1}{2}}\|_{0,h}^2 - \frac{a\theta\epsilon_0}{2\tau_v \omega_v^2} \|\overline{\sigma}_h^{n+\frac{1}{2}}\|_{0,h}^2, \tag{5.19}$$

where for all $n = 0, 1, 2, \dots, N$, the discrete (non-negative) energy is defined as

$$\begin{aligned} \mathcal{E}_{h,\text{LF}}^n := & \frac{1}{2} \left(\mu_0 \|\overline{H}_h^n\|_{\frac{1}{2},h}^2 + \epsilon_0 \epsilon_\infty \left\langle E_h^n, \left(I_h + \frac{c_\infty^2 \Delta t^2}{4} \tilde{\mathcal{D}}_h^{(2M)} \circ \mathcal{D}_h^{(2M)} \right) E_h^n \right\rangle_{0,h} \right) + \frac{\epsilon_0}{\epsilon_d} \|P_h^n\|_{0,h}^2 \\ & + \frac{\epsilon_0}{\omega_p^2} \|J_h^n\|_{0,h}^2 + \frac{a\epsilon_0}{2} (3 - 4\theta) \|(E_h^n)^2\|_{0,h}^2 + \frac{a\theta\epsilon_0}{2} \|(E_h^n)^2 + Q_h^n\|_{0,h}^2 + \frac{a\theta\epsilon_0}{2\omega_v^2} \|\sigma_h^n\|_{0,h}^2. \end{aligned} \tag{5.20}$$

Proof Let $0 \leq j \leq I - 1$. We take the average of the Eq. (5.1a) at the time step n and $n + 1$, to get

$$\mu_0 \frac{H_{j+\frac{1}{2}}^{n+\frac{3}{2}} - H_{j+\frac{1}{2}}^{n-\frac{1}{2}}}{2\Delta t} = \left(\mathcal{D}_h^{(2M)} \overline{E}_h^{n+\frac{1}{2}} \right)_{j+\frac{1}{2}}. \tag{5.21}$$

Multiplying the Eq. (5.21) by $H_{j+\frac{1}{2}}^{n+\frac{1}{2}}$, we get

$$\mu_0 \frac{H_{j+\frac{1}{2}}^{n+\frac{3}{2}} - H_{j+\frac{1}{2}}^{n-\frac{1}{2}}}{2\Delta t} \cdot H_{j+\frac{1}{2}}^{n+\frac{1}{2}} = \left(\mathcal{D}_h^{(2M)} \overline{E}_h^{n+\frac{1}{2}} \right)_{j+\frac{1}{2}} \cdot H_{j+\frac{1}{2}}^{n+\frac{1}{2}}. \tag{5.22}$$

Multiplying the Eq. (5.1b) by $\bar{E}_j^{n+\frac{1}{2}}$ and using (5.1g), we get

$$\begin{aligned} & \frac{\epsilon_0}{\Delta t} \left(\epsilon_\infty (E_j^{n+1} - E_j^n) + (P_j^{n+1} - P_j^n) + a(1 - \theta)(Y_j^{n+1} - Y_j^n) \right. \\ & \quad \left. + a\theta(Q_j^{n+1} E_j^{n+1} - Q_j^n E_j^n) \right) \cdot \bar{E}_j^{n+\frac{1}{2}} \\ & = \left(\tilde{\mathcal{D}}_h^{(2M)} H_h^{n+\frac{1}{2}} \right)_j \cdot \bar{E}_j^{n+\frac{1}{2}}. \end{aligned} \tag{5.23}$$

Multiplying the Eq. (5.1c) by $\frac{\epsilon_0}{\epsilon_d} \bar{P}_j^{n+\frac{1}{2}}$, we get

$$\frac{P_j^{n+1} - P_j^n}{\Delta t} \cdot \frac{\epsilon_0}{\epsilon_d} \bar{P}_j^{n+\frac{1}{2}} = \frac{1}{2} (J_j^{n+1} + J_j^n) \cdot \frac{\epsilon_0}{\epsilon_d} \bar{P}_j^{n+\frac{1}{2}}. \tag{5.24}$$

Multiplying the Eq. (5.1d) by $\frac{\epsilon_0}{\omega_p^2} \bar{J}_j^{n+\frac{1}{2}}$, we get

$$\begin{aligned} & \frac{J_j^{n+1} - J_j^n}{\Delta t} \cdot \frac{\epsilon_0}{\omega_p^2} \bar{J}_j^{n+\frac{1}{2}} = \left[-\frac{1}{2\tau} (J_j^{n+1} + J_j^n) - \frac{\omega_0^2}{2} (P_j^{n+1} + P_j^n) \right. \\ & \quad \left. + \frac{\omega_p^2}{2} (E_j^{n+1} + E_j^n) \right] \cdot \frac{\epsilon_0}{\omega_p^2} \bar{J}_j^{n+\frac{1}{2}}. \end{aligned} \tag{5.25}$$

From Eq. (5.1e), multiplying by $a\theta\epsilon_0 \bar{Q}_j^{n+\frac{1}{2}}$, we get

$$\frac{Q_j^{n+1} - Q_j^n}{\Delta t} \cdot a\theta\epsilon_0 \bar{Q}_j^{n+\frac{1}{2}} = \frac{1}{2} (\sigma_j^{n+1} + \sigma_j^n) \cdot a\theta\epsilon_0 \bar{Q}_j^{n+\frac{1}{2}}. \tag{5.26}$$

Finally, multiplying the Eq. (5.1f) by $\frac{a\theta\epsilon_0}{\omega_v^2} \bar{\sigma}_j^{n+\frac{1}{2}}$, we get

$$\begin{aligned} & \frac{\sigma_j^{n+1} - \sigma_j^n}{\Delta t} \cdot \frac{a\theta\epsilon_0}{\omega_v^2} \bar{\sigma}_j^{n+\frac{1}{2}} = \left[-\frac{1}{2\tau_v} (\sigma_j^{n+1} + \sigma_j^n) - \frac{\omega_v^2}{2} (Q_j^{n+1} + Q_j^n) \right. \\ & \quad \left. + \omega_v^2 E_j^n E_j^{n+1} \right] \cdot \frac{a\theta\epsilon_0}{\omega_v^2} \bar{\sigma}_j^{n+\frac{1}{2}}. \end{aligned} \tag{5.27}$$

Summing (5.22)-(5.27) over all mesh points on the dual (for H_h) and primal (for $E_h, D_h, P_h, J_h, \sigma_h, Q_h$) grids, multiplying by h , using (5.1c) again and simplifying, we get

$$\begin{aligned} & \frac{1}{2\Delta t} \left[\mu_0 \left\langle H_h^{n+\frac{3}{2}}, H_h^{n+\frac{1}{2}} \right\rangle_{\frac{1}{2},h} + \epsilon_0 \epsilon_\infty \|E_h^{n+1}\|_{0,h}^2 + \frac{3}{2} \epsilon_0 a(1 - \theta) \|(E_h^{n+1})^2\|_{0,h}^2 \right. \\ & \quad \left. + a\theta\epsilon_0 \left\langle Q_h^{n+1}, (E_h^{n+1})^2 \right\rangle_{0,h} \right. \\ & \quad \left. + \frac{\epsilon_0}{\epsilon_d} \|P_h^{n+1}\|_{0,h}^2 + \frac{\epsilon_0}{\omega_p^2} \|J_h^{n+1}\|_{0,h}^2 + a\theta\epsilon_0 \|Q_h^{n+1}\|_{0,h}^2 + \frac{a\theta\epsilon_0}{\omega_v^2} \|\sigma_h^{n+1}\|_{0,h}^2 \right] \\ & = \frac{1}{2\Delta t} \left[\mu_0 \left\langle H_h^{n-\frac{1}{2}}, H_h^{n+\frac{1}{2}} \right\rangle_{\frac{1}{2},h} + \epsilon_0 \epsilon_\infty \|E_h^n\|_{0,h}^2 \right] \end{aligned}$$

$$\begin{aligned}
 &+ \frac{3}{2} \epsilon_0 a (1 - \theta) \| (E_h^n)^2 \|_{0,h}^2 + a \theta \epsilon_0 \langle Q_h^n, (E_h^n)^2 \rangle_{0,h} \\
 &+ \frac{\epsilon_0}{\epsilon_d} \| P_h^n \|_{0,h}^2 + \frac{\epsilon_0}{\omega_p^2} \| J_h^n \|_{0,h}^2 + a \theta \epsilon_0 \| Q_h^n \|_{0,h}^2 + \frac{a \theta \epsilon_0}{\omega_v^2} \| \sigma_h^n \|_{0,h}^2 \Big] \\
 &- \frac{\epsilon_0}{4 \tau \omega_p^2} \| J_h^{n+1} + J_h^n \|_{0,h}^2 - \frac{a \theta \epsilon_0}{4 \tau \omega_v^2} \| \sigma_h^{n+1} + \sigma_h^n \|_{0,h}^2 \\
 &+ a \theta \epsilon_0 \left\langle \frac{1}{2} (\sigma_h^{n+1} + \sigma_h^n), E_h^n E_h^{n+1} \right\rangle_{0,h} - \frac{a \theta \epsilon_0}{2} \left\langle \frac{Q_h^{n+1} - Q_h^n}{\Delta t}, E_h^n E_h^{n+1} \right\rangle_{0,h} \\
 &+ h \left[\sum_{j=0}^{I-1} \frac{1}{2} (\mathcal{D}_h^{(2M)} E_h^{n+1} + \mathcal{D}_h^{(2M)} E_h^n)_{j+\frac{1}{2}} H_{j+\frac{1}{2}}^{n+\frac{1}{2}} + \sum_{j=0}^{I-1} (\tilde{\mathcal{D}}_h^{(2M)} H_h^{n+\frac{1}{2}})_j \bar{E}_j^{n+\frac{1}{2}} \right].
 \end{aligned} \tag{5.28}$$

Using Eqs. (5.1e) and (5.1f) we manipulate the following inner products in Eq. (5.28) as

$$\begin{aligned}
 &a \theta \epsilon_0 \left\langle \frac{1}{2} (\sigma_h^{n+1} + \sigma_h^n), E_h^n E_h^{n+1} \right\rangle_{0,h} - \frac{a \theta \epsilon_0}{2} \left\langle \frac{Q_h^{n+1} - Q_h^n}{\Delta t}, E_h^n E_h^{n+1} \right\rangle_{0,h} \\
 &= \frac{a \theta \epsilon_0}{2} \left\langle \frac{1}{2} (\sigma_h^{n+1} + \sigma_h^n), E_h^n E_h^{n+1} \right\rangle_{0,h} \\
 &= \frac{a \theta \epsilon_0}{2} \left\langle \frac{1}{2} (\sigma_h^{n+1} + \sigma_h^n), \frac{\sigma_j^{n+1} - \sigma_j^n}{\omega_v^2 \Delta t} \right\rangle_{0,h} \\
 &+ \frac{1}{2 \tau \omega_v^2} (\sigma_j^{n+1} + \sigma_j^n) + \frac{1}{2} (Q_j^{n+1} + Q_j^n) \Big]_{0,h} \\
 &= \frac{a \theta \epsilon_0}{4 \omega_v^2 \Delta t} (\| \sigma_h^{n+1} \|_{0,h}^2 - \| \sigma_h^n \|_{0,h}^2) + \frac{a \theta \epsilon_0}{8 \tau \omega_v^2} \| \sigma_h^{n+1} + \sigma_h^n \|_{0,h}^2 \\
 &+ \frac{a \theta \epsilon_0}{4 \Delta t} (\| Q_h^{n+1} \|_{0,h}^2 - \| Q_h^n \|_{0,h}^2).
 \end{aligned} \tag{5.29}$$

Using the result (5.29), Eq. (5.28) can be rewritten as

$$\begin{aligned}
 &\frac{1}{\Delta t} (\mathcal{E}_{h,\text{LF}}^{n+1} - \mathcal{E}_{h,\text{LF}}^n) = - \frac{\epsilon_0}{4 \tau \omega_p^2} \| J_h^{n+1} + J_h^n \|_{0,h}^2 - \frac{a \theta \epsilon_0}{8 \tau \omega_v^2} \| \sigma_h^{n+1} + \sigma_h^n \|_{0,h}^2 \\
 &+ h \left[\sum_{j=0}^{I-1} \frac{1}{2} (\mathcal{D}_h^{(2M)} E_h^{n+1} + \mathcal{D}_h^{(2M)} E_h^n)_{j+\frac{1}{2}} H_{j+\frac{1}{2}}^{n+\frac{1}{2}} \right. \\
 &\left. + \sum_{j=0}^{I-1} \frac{1}{2} (\tilde{\mathcal{D}}_h^{(2M)} H_h^{n+\frac{1}{2}})_j (E_j^{n+1} + E_j^n) \right],
 \end{aligned} \tag{5.30}$$

where $\mathcal{E}_{h,\text{LF}}^n$ is defined as

$$\begin{aligned}
 \mathcal{E}_{h,\text{LF}}^n &= \frac{1}{2} (\mu_0 \langle H_h^{n-\frac{1}{2}}, H_h^{n+\frac{1}{2}} \rangle_{\frac{1}{2},h} + \epsilon_0 \epsilon_\infty \| E_h^n \|_{0,h}^2) \\
 &+ \frac{3}{2} \epsilon_0 a (1 - \theta) \| (E_h^n)^2 \|_{0,h}^2 + a \theta \epsilon_0 \langle Q_h^n, (E_h^n)^2 \rangle_{0,h} \\
 &+ \frac{\epsilon_0}{\epsilon_d} \| P_h^n \|_{0,h}^2 + \frac{\epsilon_0}{\omega_p^2} \| J_h^n \|_{0,h}^2 + \frac{a \theta \epsilon_0}{2} \| Q_h^n \|_{0,h}^2 + \frac{a \theta \epsilon_0}{2 \omega_v^2} \| \sigma_h^n \|_{0,h}^2.
 \end{aligned} \tag{5.31}$$

Using Lemma 5.1, from (5.30) we obtain

$$\mathcal{E}_{h,\text{LF}}^{n+1} = \mathcal{E}_{h,\text{LF}}^n - \frac{\epsilon_0 \Delta t}{4\tau\omega_p^2} \|J_h^{n+1} + J_h^n\|_{0,h}^2 - \frac{a\theta\epsilon_0\Delta t}{8\tau_v\omega_v^2} \|\sigma_h^{n+1} + \sigma_h^n\|_{0,h}^2. \tag{5.32}$$

Next, we simplify terms of the Eq. (5.31). First, we have that

$$\begin{aligned} & \frac{3}{2}\epsilon_0 a(1-\theta)\|(E_h^n)^2\|_{0,h}^2 + a\theta\epsilon_0\langle Q_h^n, (E_h^n)^2 \rangle_{0,h} + \frac{a\theta\epsilon_0}{2} \|Q_h^n\|_{0,h}^2 \\ &= \frac{a\epsilon_0}{2}(3-4\theta)\|(E_h^n)^2\|_{0,h}^2 + \frac{a\theta\epsilon_0}{2} \|(E_h^n)^2 + Q_h^n\|_{0,h}^2. \end{aligned} \tag{5.33}$$

Second, by applying the parallelogram law we have

$$\begin{aligned} \langle H_h^{n-\frac{1}{2}}, H_h^{n+\frac{1}{2}} \rangle_{\frac{1}{2},h} &= \frac{1}{4} \left[\|H_h^{n+\frac{1}{2}} + H_h^{n-\frac{1}{2}}\|_{\frac{1}{2},h}^2 - \|H_h^{n+\frac{1}{2}} - H_h^{n-\frac{1}{2}}\|_{\frac{1}{2},h}^2 \right] \\ &= \|\overline{H}_h^n\|_{\frac{1}{2},h}^2 - \frac{\Delta t^2}{4\mu_0^2} \|\mathcal{D}_h^{(2M)} E_h^n\|_{\frac{1}{2},h}^2. \end{aligned} \tag{5.34}$$

Lastly, using Eq. (5.34), we have

$$\begin{aligned} & \mu_0 \langle H_h^{n-\frac{1}{2}}, H_h^{n+\frac{1}{2}} \rangle_{\frac{1}{2},h} + \epsilon_0 \epsilon_\infty \|E_h^n\|_{0,h}^2 \\ &= \mu_0 \|\overline{H}_h^n\|_{\frac{1}{2},h}^2 - \frac{\Delta t^2}{4\mu_0} \|\mathcal{D}_h^{(2M)} E_h^n\|_{\frac{1}{2},h}^2 + \epsilon_0 \epsilon_\infty \|E_h^n\|_{0,h}^2 \\ &= \mu_0 \|\overline{H}_h^n\|_{\frac{1}{2},h}^2 + \epsilon_0 \epsilon_\infty \left[\langle E_h^n, E_h^n \rangle_{0,h} - \frac{\Delta t^2}{4\epsilon_0 \epsilon_\infty \mu_0} \langle \mathcal{D}_h^{(2M)} E_h^n, \mathcal{D}_h^{(2M)} E_h^n \rangle_{\frac{1}{2},h} \right] \\ &= \mu_0 \|\overline{H}_h^n\|_{\frac{1}{2},h}^2 + \epsilon_0 \epsilon_\infty \left[\langle E_h^n, E_h^n \rangle_{0,h} + \frac{\Delta t^2}{4\epsilon_0 \epsilon_\infty \mu_0} \langle E_h^n, \tilde{\mathcal{D}}_h^{(2M)} \mathcal{D}_h^{(2M)} E_h^n \rangle_{0,h} \right] \\ &= \mu_0 \|\overline{H}_h^n\|_{\frac{1}{2},h}^2 + \epsilon_0 \epsilon_\infty \left\langle E_h^n, \left(I_h + \frac{c_\infty^2 \Delta t^2}{4} \tilde{\mathcal{D}}_h^{(2M)} \circ \mathcal{D}_h^{(2M)} \right) E_h^n \right\rangle_{0,h}. \end{aligned} \tag{5.35}$$

Substituting Eqs. (5.33) and (5.35) into the discrete energy definition (5.31), we obtain the alternate definition of the discrete energy, $\mathcal{E}_{h,\text{LF}}^n$, given in (5.20). Applying Theorem 5.2, the discrete energy, $\mathcal{E}_{h,\text{LF}}^n$, is positive and satisfies the discrete energy identity (5.32) under the CFL conditions given in (5.18), which are obtained from Theorem 5.2. \square

Remark 5.1 Since our discretization staggers the electric and magnetic fields in space and time, our methods are similar to other leap-frog FDTD methods for Maxwell’s equations in the literature. However, the time discretization that we employ is different from what has been used in the literature (see for e.g. [16]) to discretize (2, 2) and (2, 4) schemes. The reason for our choice of a different time discretization from what is available in the literature, has to do with constructing fully discrete FDTD methods that satisfy discrete versions of the energy decay Theorem 3.1. It is unclear whether the FDTD method used in, for example [16], has an associated discrete energy decay.

Remark 5.2 In [4] it was shown that the (2, 4) leap-frog FDTD method for a linear Lorentz model is superior to the (2, 2) leap-frog FDTD method from the perspective of numerical dispersion. However, beyond fourth order in space there was not much more benefit in reduction of dispersion. To get additional reduction in numerical dispersion we need to consider higher order methods in time, which is a nontrivial extension and will be investigated in a future paper.

6 Fully Discrete Trapezoidal FDTD Methods

In this section, we construct fully discrete FDTD schemes for the discretization of the system (3.1)–(3.2) using the trapezoidal time integrator. The main goal here is to produce schemes that are unconditionally stable. We call such schemes $(2, 2M)$ trapezoidal FDTD schemes. They are constructed by applying the high order $2M$ discretizations in space outlined in Sect. 4 and the second order trapezoidal time integrator. We continue to stagger the electric and magnetic fields in space as in the leap frog FDTD methods, i.e., the magnetic field is defined in the space $V_{\frac{1}{2},h}$. However, we do not stagger the fields in time. Thus, the magnetic field, like the other fields, is now defined at integer time steps (primal in time), $n = 0, 1, \dots, N$, rather than at integer plus half time steps. Our fully discrete $(2, 2M)$ trapezoidal FDTD schemes for the discretization of the nonlinear Maxwell problem are given as follows.

Assume $D_h^0, E_h^0, P_h^0, J_h^0, Q_h^0, \sigma_h^0, Y_h^0 \in V_{0,h}$ and $H_h^0 \in V_{\frac{1}{2},h}$ are given. Then $\forall n \in \mathbb{N}$, with $0 < n \leq N$, find $D_h^n, E_h^n, P_h^n, J_h^n, Q_h^n, \sigma_h^n, Y_h^n \in V_{0,h}$ and $H_h^n \in V_{\frac{1}{2},h}$, so that $\forall j$ with $0 \leq j \leq I$ we have

$$\mu_0 \frac{H_{j+\frac{1}{2}}^{n+1} - H_{j+\frac{1}{2}}^n}{\Delta t} = \frac{1}{2} \left(\mathcal{D}_h^{(2M)} E_h^{n+1} + \mathcal{D}_h^{(2M)} E_h^n \right)_{j+\frac{1}{2}}, \tag{6.1a}$$

$$\frac{D_j^{n+1} - D_j^n}{\Delta t} = \frac{1}{2} \left(\tilde{\mathcal{D}}_h^{(2M)} H_h^{n+1} + \tilde{\mathcal{D}}_h^{(2M)} H_h^n \right)_j, \tag{6.1b}$$

$$\frac{P_j^{n+1} - P_j^n}{\Delta t} = \frac{1}{2} \left(J_j^{n+1} + J_j^n \right), \tag{6.1c}$$

$$\frac{J_j^{n+1} - J_j^n}{\Delta t} = -\frac{1}{2\tau} \left(J_j^{n+1} + J_j^n \right) - \frac{\omega_0^2}{2} \left(P_j^{n+1} + P_j^n \right) + \frac{\omega_p^2}{2} \left(E_j^{n+1} + E_j^n \right), \tag{6.1d}$$

$$\frac{Q_j^{n+1} - Q_j^n}{\Delta t} = \frac{1}{2} \left(\sigma_j^{n+1} + \sigma_j^n \right), \tag{6.1e}$$

$$\frac{\sigma_j^{n+1} - \sigma_j^n}{\Delta t} = -\frac{1}{2\tau_v} \left(\sigma_j^{n+1} + \sigma_j^n \right) - \frac{\omega_v^2}{2} \left(Q_j^{n+1} + Q_j^n \right) + \omega_v^2 E_j^n E_j^{n+1}, \tag{6.1f}$$

$$D_j^{n+1} = \epsilon_0 \left(\epsilon_\infty E_j^{n+1} + P_j^{n+1} + a(1 - \theta) Y_j^{n+1} + a\theta Q_j^{n+1} E_j^{n+1} \right), \tag{6.1g}$$

where

$$Y_j^{n+1} = Y_j^n + \frac{3}{2} \left((E_j^{n+1})^2 + (E_j^n)^2 \right) \left(E_j^{n+1} - E_j^n \right). \tag{6.2}$$

As opposed to the $(2, 2M)$ order leap frog FDTD schemes, the trapezoidal FDTD schemes are unconditionally stable due to the fully implicit nature of the time discretization. We prove this unconditional stability in the theorem below.

Theorem 6.1 Assume $\theta \in [0, \frac{3}{4}]$, and $0 \leq n \leq N$. Let $H_h^n \in V_{\frac{1}{2},h}$, $E_h^n, P_h^n, J_h^n, \sigma_h^n, Q_h^n \in V_{0,h}$. The $(2, 2M)$ order trapezoidal FDTD schemes (6.1) are unconditionally stable and satisfy the energy identity

$$\frac{\mathcal{E}_{h, \text{Trap}}^{n+1} - \mathcal{E}_{h, \text{Trap}}^n}{\Delta t} = -\frac{\epsilon_0}{\tau \omega_p^2} \|\overline{J}_h^{n+\frac{1}{2}}\|_{0,h}^2 - \frac{a\epsilon_0\theta}{2\tau_v\omega_v^2} \|\overline{\sigma}_h^{n+\frac{1}{2}}\|_{0,h}^2, \tag{6.3}$$

where, the discrete energy is defined as

$$\begin{aligned} \mathcal{E}_{h, \text{Trap}}^n := & \frac{1}{2} \left(\mu_0 \|H_h^n\|_{0,h}^2 + \epsilon_0 \epsilon_\infty \|E_h^n\|_{0,h}^2 + \frac{a\epsilon_0}{2} (3 - 4\theta) \|(E_h^n)^2\|_{0,h}^2 \right. \\ & \left. + \frac{a\epsilon_0\theta}{2} \|(E_h^n)^2 + Q_h^n\|_{0,h}^2 + \frac{\epsilon_0}{\epsilon_d} \|P_h^n\|_{0,h}^2 + \frac{\epsilon_0}{\omega_p^2} \|J_h^n\|_{0,h}^2 + \frac{a\epsilon_0\theta}{2\omega_v^2} \|\sigma_h^n\|_{0,h}^2 \right). \end{aligned} \tag{6.4}$$

Proof Multiplying the Eq. (6.1a) by $\overline{H}_j^{n+\frac{1}{2}}$, we get

$$\mu_0 \frac{H_{j+\frac{1}{2}}^{n+1} - H_{j+\frac{1}{2}}^n}{\Delta t} \cdot \overline{H}_j^{n+\frac{1}{2}} = \frac{1}{2} \left(\mathcal{D}_h^{(2M)} E_h^{n+1} + \mathcal{D}_h^{(2M)} E_h^n \right)_{j+\frac{1}{2}} \cdot \overline{H}_j^{n+\frac{1}{2}}. \tag{6.5}$$

From Eq. (6.1b), multiplying by $\overline{E}_j^{n+\frac{1}{2}}$ and using (6.1g), we get

$$\begin{aligned} & \frac{\epsilon_0}{\Delta t} \left(\epsilon_\infty (E_j^{n+1} - E_j^n) + (P_j^{n+1} - P_j^n) + a(1 - \theta)(Y_j^{n+1} - Y_j^n) \right. \\ & \quad \left. + a\theta(Q_j^{n+1} E_j^{n+1} - Q_j^n E_j^n) \right) \cdot \overline{E}_j^{n+\frac{1}{2}} \\ & = \left(\tilde{\mathcal{D}}_h^{(2M)} H_h^{n+\frac{1}{2}} \right)_j \cdot \overline{E}_j^{n+\frac{1}{2}}. \end{aligned} \tag{6.6}$$

Next, multiplying the Eq. (6.1c) by $\frac{\epsilon_0}{\epsilon_d} \overline{P}_j^{n+\frac{1}{2}}$, we have

$$\frac{P_j^{n+1} - P_j^n}{\Delta t} \cdot \frac{\epsilon_0}{\epsilon_d} \overline{P}_j^{n+\frac{1}{2}} = \frac{1}{2} \left(J_j^{n+1} + J_j^n \right) \cdot \frac{\epsilon_0}{\epsilon_d} \overline{P}_j^{n+\frac{1}{2}}. \tag{6.7}$$

From Eq. (6.1d), multiplying by $\frac{\epsilon_0}{\omega_p^2} \overline{J}_j^{n+\frac{1}{2}}$, we obtain

$$\begin{aligned} \frac{J_j^{n+1} - J_j^n}{\Delta t} \cdot \frac{\epsilon_0}{\omega_p^2} \overline{J}_j^{n+\frac{1}{2}} = & \left[-\frac{1}{2\tau} \left(J_j^{n+1} + J_j^n \right) - \frac{\omega_0^2}{2} \left(P_j^{n+1} + P_j^n \right) \right. \\ & \left. + \frac{\omega_p^2}{2} \left(E_j^{n+1} + E_j^n \right) \right] \cdot \frac{\epsilon_0}{\omega_p^2} \overline{J}_j^{n+\frac{1}{2}}. \end{aligned} \tag{6.8}$$

Multiplying the Eq. (6.1e) by $\epsilon_0 a \theta \overline{Q}_j^{n+\frac{1}{2}}$, we get

$$\frac{Q_j^{n+1} - Q_j^n}{\Delta t} \cdot \epsilon_0 a \theta \overline{Q}_j^{n+\frac{1}{2}} = \frac{1}{2} \left(\sigma_j^{n+1} + \sigma_j^n \right) \cdot \epsilon_0 a \theta \overline{Q}_j^{n+\frac{1}{2}}. \tag{6.9}$$

Lastly, multiplying the Eq. (6.1f) by $\frac{a\theta\epsilon_0}{\omega_v^2} \overline{\sigma}_j^{n+\frac{1}{2}}$, we get

$$\begin{aligned} \frac{\sigma_j^{n+1} - \sigma_j^n}{\Delta t} \cdot \frac{a\theta\epsilon_0}{\omega_v^2} \overline{\sigma}_j^{n+\frac{1}{2}} = & \left[-\frac{1}{2\tau_v} \left(\sigma_j^{n+1} + \sigma_j^n \right) - \frac{\omega_v^2}{2} \left(Q_j^{n+1} + Q_j^n \right) \right. \\ & \left. + \omega_v^2 E_j^n E_j^{n+1} \right] \cdot \frac{a\theta\epsilon_0}{\omega_v^2} \overline{\sigma}_j^{n+\frac{1}{2}}. \end{aligned} \tag{6.10}$$

Adding Eqs. (6.5)–(6.10), taking sums over all mesh points on either the dual (magnetic field) or primary (all other fields) grids, multiplying by h and simplifying, we get

$$\begin{aligned}
 & \frac{1}{2\Delta t} \left[\mu_0 \|H_h^{n+1}\|_{\frac{1}{2},h}^2 + \epsilon_0 \epsilon_\infty \|E_h^{n+1}\|_{0,h}^2 \right. \\
 & \quad + \frac{3}{2} \epsilon_0 a (1 - \theta) \| (E_h^{n+1})^2 \|_{0,h}^2 + \epsilon_0 a \theta \left\langle Q_h^{n+1}, (E_h^{n+1})^2 \right\rangle_{0,h} \\
 & \quad + \frac{\epsilon_0}{\epsilon_d} \|P_h^{n+1}\|_{0,h}^2 + \frac{\epsilon_0}{\omega_p^2} \|J_h^{n+1}\|_{0,h}^2 + \epsilon_0 a \theta \|Q_h^{n+1}\|_{0,h}^2 + \frac{a\theta\epsilon_0}{\omega_v^2} \|\sigma_h^{n+1}\|_{0,h}^2 \left. \right] \\
 & = \frac{1}{2\Delta t} \left[\mu_0 \|H_h^n\|_{\frac{1}{2},h}^2 + \epsilon_0 \epsilon_\infty \|E_h^n\|_{0,h}^2 + \frac{3}{2} \epsilon_0 a (1 - \theta) \| (E_h^n)^2 \|_{0,h}^2 + \epsilon_0 a \theta \left\langle Q_h^n, (E_h^n)^2 \right\rangle_{0,h} \right. \\
 & \quad + \frac{\epsilon_0}{\epsilon_d} \|P_h^n\|_{0,h}^2 + \frac{\epsilon_0}{\omega_p^2} \|J_h^n\|_{0,h}^2 + \epsilon_0 a \theta \|Q_h^n\|_{0,h}^2 + \frac{a\theta\epsilon_0}{\omega_v^2} \|\sigma_h^n\|_{0,h}^2 \left. \right] \\
 & \quad + a\epsilon_0 \theta \left\langle \frac{1}{2} (\sigma_h^{n+1} + \sigma_h^n), E_h^n E_h^{n+1} \right\rangle_{0,h} \\
 & \quad - \frac{\epsilon_0}{4\tau\omega_p^2} \|J_h^{n+1} + J_h^n\|_{0,h}^2 - \frac{a\theta\epsilon_0}{4\tau_v\omega_v^2} \|\sigma_h^{n+1} + \sigma_h^n\|_{0,h}^2 - \frac{\epsilon_0 a \theta}{2} \left\langle \frac{Q_h^{n+1} - Q_h^n}{\Delta t}, E_h^n E_h^{n+1} \right\rangle_{0,h} \\
 & \quad + h \left[\sum_{j=0}^{I-1} \frac{1}{4} \left(\mathcal{D}_h^{(2M)} E_h^{n+1} + \mathcal{D}_h^{(2M)} E_h^n \right)_{j+\frac{1}{2}} \left(H_{j+\frac{1}{2}}^{n+1} + H_{j+\frac{1}{2}}^n \right) \right] \\
 & \quad + h \left[\sum_{j=0}^{I-1} \frac{1}{4} \left(\tilde{\mathcal{D}}_h^{(2M)} H_h^{n+1} + \tilde{\mathcal{D}}_h^{(2M)} H_h^n \right)_j \left(E_j^{n+1} + E_j^n \right) \right].
 \end{aligned} \tag{6.11}$$

From (5.29) and (5.33), and using the definition of the discrete energy (6.4), the Eq. (6.11) can be rewritten as

$$\begin{aligned}
 \frac{1}{\Delta t} \mathcal{E}_{h,\text{Trap}}^{n+1} & = \frac{1}{\Delta t} \mathcal{E}_{h,\text{Trap}}^n - \frac{\epsilon_0}{4\tau\omega_p^2} \|J_h^{n+1} + J_h^n\|_{0,h}^2 - \frac{a\epsilon_0\theta}{8\tau_v\omega_v^2} \|\sigma_h^{n+1} + \sigma_h^n\|_{0,h}^2 \\
 & \quad + h \sum_{j=0}^{I-1} \frac{1}{4} \left(\mathcal{D}_h^{(2M)} E_h^{n+1} + \mathcal{D}_h^{(2M)} E_h^n \right)_{j+\frac{1}{2}} \left(H_{j+\frac{1}{2}}^{n+1} + H_{j+\frac{1}{2}}^n \right) \\
 & \quad + h \sum_{j=0}^{I-1} \frac{1}{4} \left(\tilde{\mathcal{D}}_h^{(2M)} H_h^{n+1} + \tilde{\mathcal{D}}_h^{(2M)} H_h^n \right)_j \left(E_j^{n+1} + E_j^n \right),
 \end{aligned} \tag{6.12}$$

By using the summation by parts Lemma 5.1, we finally obtain

$$\mathcal{E}_{h,\text{Trap}}^{n+1} = \mathcal{E}_{h,\text{Trap}}^n - \frac{\epsilon_0\Delta t}{4\tau\omega_p^2} \|J_h^{n+1} + J_h^n\|_{0,h}^2 - \frac{a\epsilon_0\theta\Delta t}{8\tau_v\omega_v^2} \|\sigma_h^{n+1} + \sigma_h^n\|_{0,h}^2, \tag{6.13}$$

which can be simplified into the energy decay result (6.3). Since this result is obtained without making any assumptions on the spatial mesh or temporal step sizes, the $(2, 2M)$ order trapezoidal FDTD schemes satisfy the discrete energy identity (6.3), for the energy (6.4) unconditionally on h and Δt . Thus, these schemes are unconditionally stable when $\theta \in [0, \frac{3}{4}]$. □

7 Fully Discrete FDTD Methods on Nonuniform Grids

In this section, we extend the fully discrete FDTD schemes constructed in Sects. 5 and 6 to a nonuniform grid. The development of the Yee scheme (leap-frog FDTD, $M = 1$) on nonuniform rectangular type grids has been studied for Maxwell’s equations in a variety of materials [36,39]. Here we present details of the construction and analysis of the fully discrete leap-frog and trapezoidal FDTD methods on a nonuniform one dimensional grid for the case $M = 1$. As done in Sect. 4, we first define below the primal, \tilde{G}_p , and dual grid, \tilde{G}_d , on nonuniform grids in (4.1) and (4.2), respectively.

Consider the computational domain $\Omega = [0, L]$. We define two staggered grids on Ω . The primal grid, \tilde{G}_p , is defined as

$$\tilde{G}_p : 0 = x_0 < x_1 < x_2 < \dots < x_{I-1} < x_I = L. \tag{7.1}$$

The dual grid, \tilde{G}_d , on Ω is defined as

$$\tilde{G}_d : x_{\frac{1}{2}} < x_{\frac{3}{2}} < x_{\frac{5}{2}} < \dots < x_{I-\frac{1}{2}}. \tag{7.2}$$

We also define $x_{\ell+\frac{1}{2}} = (x_{\ell+1} + x_\ell)/2$ for $\ell = 0, 1, \dots, I - 1$, and mesh sizes $h_\ell := x_{\ell+1} - x_\ell$ and $h_{\ell-\frac{1}{2}} := x_{\ell+\frac{1}{2}} - x_{\ell-\frac{1}{2}}$. Denote the approximations $v_\ell \approx v(x_\ell)$ and $u_{\ell+\frac{1}{2}} \approx u(x_{\ell+\frac{1}{2}})$. The corresponding norms on both grids with periodic boundary condition are given by

$$\tilde{V}_{0,h} := \{v_h := (v_\ell), 0 \leq \ell \leq I - 1, v_0 = v_I \mid \|v_h\|_{0,h}^2 = \sum_{\ell=0}^{I-1} h_{\ell-\frac{1}{2}} |v_\ell|^2 < \infty\}, \tag{7.3a}$$

$$\tilde{V}_{\frac{1}{2},h} := \left\{ u_h := \left(u_{\ell+\frac{1}{2}} \right), 0 \leq \ell \leq I - 1, u_{\frac{1}{2}} = u_{I+\frac{1}{2}} \mid \|u_h\|_{\frac{1}{2},h}^2 = \sum_{\ell=0}^{I-1} h_\ell |u_{\ell+\frac{1}{2}}|^2 < \infty \right\}. \tag{7.3b}$$

Next, we define the discrete operators

$$\mathcal{D}_x : \tilde{V}_{0,h} \rightarrow \tilde{V}_{\frac{1}{2},h}, (\mathcal{D}_x v_h)_{j+\frac{1}{2}} = \frac{v_{j+1} - v_j}{h_j}, \quad \forall v_h \in \tilde{V}_{0,h}, \tag{7.4a}$$

$$\tilde{\mathcal{D}}_x : \tilde{V}_{\frac{1}{2},h} \rightarrow \tilde{V}_{0,h}, (\tilde{\mathcal{D}}_x u_h)_j = \frac{u_{j+\frac{1}{2}} - u_{j-\frac{1}{2}}}{h_{j-\frac{1}{2}}}, \quad \forall u_h \in \tilde{V}_{\frac{1}{2},h}. \tag{7.4b}$$

Then the numerical schemes (5.1), (6.1) can be defined in the same way for $M = 1$ on such nonuniform meshes. The results in [39] can be used to establish second order convergence for the schemes. As for energy stability, we follow the same lines of the proof for Theorems 5.3 and 6.1, and obtain the following results.

Theorem 7.1 *Let $0 \leq n \leq N$. Let $H_h^{n+\frac{1}{2}} \in \tilde{V}_{\frac{1}{2},h}$, $E_h^n, P_h^n, J_h^n, \sigma_h^n, Q_h^n \in \tilde{V}_{0,h}$, and assume $\theta \in [0, \frac{3}{4}]$. Under the CFL condition*

$$\frac{c_\infty \Delta t}{\left(\min_\ell \{h_\ell\} \min_\ell \{h_{\ell-\frac{1}{2}}\} \right)^{1/2}} < 1, \tag{7.5}$$

the (2, 2) order leap-frog FDTD scheme on the nonuniform grids satisfies the discrete energy identity

$$\frac{\mathcal{E}_{h,\text{LF}}^{n+1} - \mathcal{E}_{h,\text{LF}}^n}{\Delta t} = -\frac{\epsilon_0}{\tau\omega_p^2} \|\overline{J}_h^{n+\frac{1}{2}}\|_{0,h}^2 - \frac{a\theta\epsilon_0}{2\tau_v\omega_v^2} \|\overline{\sigma}_h^{n+\frac{1}{2}}\|_{0,h}^2, \tag{7.6}$$

where for all $n = 0, 1, 2, \dots, N$, the discrete (non-negative) energy is defined as

$$\begin{aligned} \mathcal{E}_{h,\text{LF}}^n := & \frac{1}{2} \left(\mu_0 \|\overline{H}_h^n\|_{\frac{1}{2},h}^2 + \epsilon_0 \epsilon_\infty \left\langle E_h^n, \left(I_h + \frac{c_\infty^2 \Delta t^2}{4} \tilde{\mathcal{D}}_x \circ \mathcal{D}_x \right) E_h^n \right\rangle_{0,h} + \frac{\epsilon_0}{\epsilon_d} \|P_h^n\|_{0,h}^2 \right. \\ & \left. + \frac{\epsilon_0}{\omega_p^2} \|J_h^n\|_{0,h}^2 + \frac{a\epsilon_0}{2} (3 - 4\theta) \|(E_h^n)^2\|_{0,h}^2 + \frac{a\theta\epsilon_0}{2} \|(E_h^n)^2 + Q_h^n\|_{0,h}^2 + \frac{a\theta\epsilon_0}{2\omega_v^2} \|\sigma_h^n\|_{0,h}^2 \right). \end{aligned} \tag{7.7}$$

Proof Based on the norms on both grids, the approximations (5.1a) and (5.1b) can be rewritten for the case of nonuniform grids as

$$\mu_0 \frac{H_{j+\frac{1}{2}}^{n+\frac{1}{2}} - H_{j+\frac{1}{2}}^{n-\frac{1}{2}}}{\Delta t} = (\mathcal{D}_x E_h^n)_{j+\frac{1}{2}}, \tag{7.8a}$$

$$\frac{D_j^{n+1} - D_j^n}{\Delta t} = (\tilde{\mathcal{D}}_x H_h^{n+\frac{1}{2}})_j. \tag{7.8b}$$

Following the proof in Theorem 5.3, we consequently obtain the energy identity (7.6). The discrete energy, $\mathcal{E}_{h,\text{LF}}^n$, is non-negative by Cauchy–Schwarz inequality under the CFL condition for the nonuniform grids given in (7.5). \square

On the uniform grid, $\min_\ell \{h_\ell\} = \min\{h_{\ell-\frac{1}{2}}\} = h$. In this case, identity (7.5) clearly is the same as identity (5.18).

Theorem 7.2 Assume $\theta \in [0, \frac{3}{4}]$, and $0 \leq n \leq N$. Let $H_h^n \in \tilde{V}_{\frac{1}{2},h}$, $E_h^n, P_h^n, J_h^n, \sigma_h^n, Q_h^n \in \tilde{V}_{0,h}$. The (2, 2) order trapezoidal FDTD scheme on the nonuniform grids is unconditionally stable and satisfies the energy identity

$$\frac{\mathcal{E}_{h,\text{Trap}}^{n+1} - \mathcal{E}_{h,\text{Trap}}^n}{\Delta t} = -\frac{\epsilon_0}{\tau\omega_p^2} \|\overline{J}_h^{n+\frac{1}{2}}\|_{0,h}^2 - \frac{a\epsilon_0\theta}{2\tau_v\omega_v^2} \|\overline{\sigma}_h^{n+\frac{1}{2}}\|_{0,h}^2, \tag{7.9}$$

where, the discrete energy is defined as

$$\begin{aligned} \mathcal{E}_{h,\text{Trap}}^n := & \frac{1}{2} \left(\mu_0 \|H_h^n\|_{0,h}^2 + \epsilon_0 \epsilon_\infty \|E_h^n\|_{0,h}^2 + \frac{a\epsilon_0}{2} (3 - 4\theta) \|(E_h^n)^2\|_{0,h}^2 \right. \\ & \left. + \frac{a\epsilon_0\theta}{2} \|(E_h^n)^2 + Q_h^n\|_{0,h}^2 + \frac{\epsilon_0}{\epsilon_d} \|P_h^n\|_{0,h}^2 + \frac{\epsilon_0}{\omega_p^2} \|J_h^n\|_{0,h}^2 + \frac{a\epsilon_0\theta}{2\omega_v^2} \|\sigma_h^n\|_{0,h}^2 \right). \end{aligned} \tag{7.10}$$

Proof As done in the proof of Theorem 7.1, we need to rewrite the approximations (6.1a) and (6.1b) for the case of nonuniform grids and then proceed with the proof of energy stability in a similar manner to the proof of Theorem 6.1. \square

The extension of the fully discrete leap-frog and trapezoidal schemes for $M > 1$ to nonuniform grids is nontrivial, particularly for maintaining high order accuracy on dual meshes. Such extensions will be investigated in our future work.

8 Numerical Simulations

In this section, we present results of numerical simulations that illustrate the theoretical results that we have developed in the paper. For our numerical simulations we use a non-dimensionalized verion of the nonlinear Maxwell model (3.1)–(3.2) considered in this paper. We scale the time and space variables by a reference time scale t_0 and reference distance scale x_0 , respectively, with $x_0 = ct_0$ and $c = 1/\sqrt{\mu_0\epsilon_0}$ as

$$\tilde{x} = \frac{x}{x_0}, \quad \tilde{t} = \frac{t}{t_0}. \tag{8.1}$$

We also use a reference electric field E_0 to scale parameters and field variables. The scaled representation of variable or parameter V is denoted as \tilde{V} . The non-dimensionalized parameters and variables are given as

$$\tilde{E} = \frac{1}{E_0}E, \quad \tilde{H} = \sqrt{\frac{\mu_0}{\epsilon_0}} \frac{1}{E_0}H, \quad \tilde{D} = \frac{1}{\epsilon_0 E_0}D, \quad \tilde{P} = \frac{1}{E_0}P, \quad \tilde{J} = \frac{t_0}{E_0}J, \tag{8.2}$$

$$\tilde{Q} = \frac{1}{E_0^2}Q, \quad \tilde{\sigma} = \frac{t_0}{E_0^2}\sigma, \quad \tilde{a} = E_0^2a, \quad \tilde{\omega}_0 = t_0\omega_0, \quad \tilde{\omega}_p = t_0\omega_p, \tag{8.3}$$

$$\tilde{\omega}_v = t_0\omega_v, \quad \frac{1}{\tilde{\tau}} = \frac{t_0}{\tau}, \quad \frac{1}{\tilde{\tau}_v} = \frac{t_0}{\tau_v}. \tag{8.4}$$

The Maxwell’s system (3.1)–(3.2) is then converted into dimensionless form as

$$\frac{\partial \tilde{H}}{\partial \tilde{t}} = \frac{\partial \tilde{E}}{\partial \tilde{x}}, \tag{8.5a}$$

$$\frac{\partial \tilde{D}}{\partial \tilde{t}} = \frac{\partial \tilde{H}}{\partial \tilde{x}}, \tag{8.5b}$$

$$\frac{\partial \tilde{P}}{\partial \tilde{t}} = \tilde{J}, \tag{8.5c}$$

$$\frac{\partial \tilde{J}}{\partial \tilde{t}} = -\frac{1}{\tilde{\tau}}\tilde{J} - \tilde{\omega}_0^2\tilde{P} + \tilde{\omega}_p^2\tilde{E}, \tag{8.5d}$$

$$\frac{\partial \tilde{Q}}{\partial \tilde{t}} = \tilde{\sigma}, \tag{8.5e}$$

$$\frac{\partial \tilde{\sigma}}{\partial \tilde{t}} = -\frac{1}{\tilde{\tau}_v}\tilde{\sigma} - \tilde{\omega}_v^2\tilde{Q} + \tilde{\omega}_v^2\tilde{E}^2, \tag{8.5f}$$

along with the constitutive law

$$\tilde{D} = \epsilon_\infty\tilde{E} + \tilde{a}(1 - \theta)\tilde{E}^3 + \tilde{P} + \tilde{a}\theta\tilde{Q}\tilde{E}, \tag{8.6}$$

The energy $\tilde{\mathcal{E}}_\theta(\tilde{t})$ corresponding to the dimensionless Maxwell’s equations (8.5)–(8.6) defined as

$$\frac{d}{d\tilde{t}} \tilde{\mathcal{E}}_\theta(\tilde{t}) = - \int_\Omega \left(\frac{1}{\tilde{\tau}\tilde{\omega}_p^2} \tilde{J}^2 + \frac{\tilde{a}\theta}{2\tilde{\tau}_v\tilde{\omega}_v^2} \tilde{\sigma}^2 \right) d\tilde{x}, \tag{8.7}$$

satisfies the relation

$$\begin{aligned} \tilde{\mathcal{E}}_\theta(\tilde{t}) := & \frac{1}{2} \int_{\Omega} \left(\tilde{H}^2 + \epsilon_\infty \tilde{E}^2 + \frac{1}{\epsilon_d} \tilde{P}^2 + \frac{1}{\tilde{\omega}_p^2} \tilde{J}^2 \right. \\ & \left. + \frac{\tilde{a}\theta}{2\tilde{\omega}_v^2} \tilde{\sigma}^2 + \frac{\tilde{a}\theta}{2} (\tilde{Q} + \tilde{E}^2) + \frac{\tilde{a}}{2} (3 - 4\theta) \tilde{E}^4 \right) d\tilde{x}. \end{aligned}$$

8.1 Traveling Wave Solutions

In this section, we consider a traveling wave problem [43] modeled by the dimensionless Maxwell’s equations (8.5)–(8.6) with no damping in the linear Lorentz model, i.e. $1/\tilde{\tau} = 0$, and no Raman scattering, i.e. $\theta = 0$. The nonlinearity in the constitutive laws appears only in the instantaneous intensity-dependent Kerr response. Here we make the traveling wave assumption on the electric field, i.e. $\tilde{E}(\tilde{t}, \tilde{x}) = \tilde{E}(\tilde{\xi})$, where $\tilde{\xi} = \tilde{x} - v\tilde{t}$, and similar assumptions for the fields \tilde{H} , \tilde{J} , \tilde{P} and \tilde{D} . Substituting this solution ansatz into the dimensionless nonlinear Maxwell system (8.5)–(8.6), we obtain the following system of nonlinear ODEs.

$$\frac{d\tilde{E}}{d\tilde{\xi}} = \tilde{W}, \tag{8.8a}$$

$$\frac{d\tilde{W}}{d\tilde{\xi}} = \frac{6\tilde{a}v^2\tilde{E}\tilde{W}^2 - \tilde{\omega}_0^2 \left(\frac{1}{v^2} - \epsilon_s \right) + \tilde{a}\tilde{\omega}_0^2\tilde{E}^3}{1 - \epsilon_\infty v^2 - 3\tilde{a}\tilde{E}^2 v^2}. \tag{8.8b}$$

In Fig. 1, we plot the behavior of solutions of system (8.8) in the phase plane (left), obtained numerically by solving the system (8.8). As seen in the phase plot in Fig. 1(left), the system (8.8) has three stationary solutions or fixed points: A center at (0,0), and two hyperbolic unstable fixed points of equal amplitude but different sign on the $\tilde{Y} = 0$ axis. Around the center at the origin we see closed elliptic trajectories corresponding to linear oscillating solutions. The upper heteroclinic trajectory connecting the left hyperbolic fixed point to the right hyperbolic fixed point forms a *kink* solution, while the lower heteroclinic trajectory connecting the right hyperbolic fixed point with the left forms an *antikink* solution.

We numerically solve the ODE system (8.8) with initial conditions $(\tilde{E}(0), \tilde{Y}(0)) = (0, Y_0)$, and Y_0 large enough to produce a nonlinear solution that is a train of kink–antikink nonlinear waves. In the phase plane plot this represents a solution path that closely follows the heteroclinic orbits within their closure [43]. This solution \tilde{E} of the system (8.8) is plotted on the right in Fig. 1.

We use this example as an accuracy test for the (2, 2M) leap-frog and trapezoidal FDTD methods, and reproduce the solution of system (8.8) shown in Fig. 1 (right) using the non-dimensionalized Maxwell system (8.5)–(8.6) discretized using either the leap-frog or the trapezoidal FDTD schemes for $M = 1, 2, 3$. We first describe the implementation of our numerical schemes on a uniform spatial mesh with periodic boundary conditions.

8.1.1 Implementation of (2, 2M) Leap-Frog Scheme

Let $M \in \mathbb{N}$. The fully discrete equations for the (2, 2M) leap-frog FDTD scheme for the dimensionless Maxwell system (8.5)–(8.6) for the travelling wave problem are given as

$$\tilde{H}_{j+\frac{1}{2}}^{n+\frac{1}{2}} = \tilde{H}_{j+\frac{1}{2}}^{n-\frac{1}{2}} + \Delta\tilde{t} \left(\mathcal{D}_h^{(2M)} \tilde{E}_h^n \right)_{j+\frac{1}{2}}, \tag{8.9a}$$

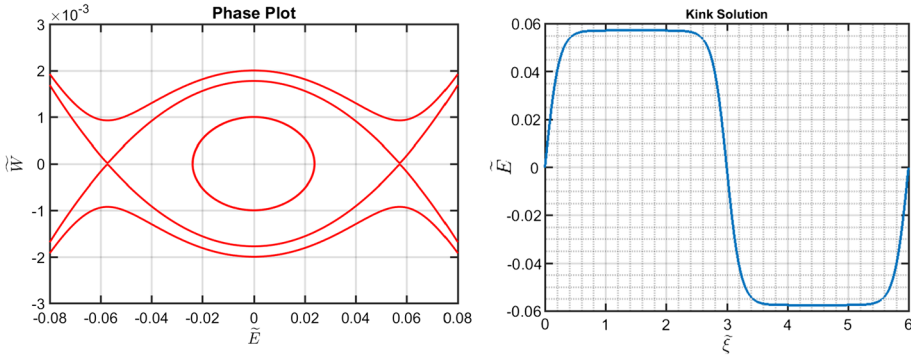


Fig. 1 (Left): phase plane flow from the scaled Eq. (8.8). (Right): the solution \tilde{E} of system (8.8) corresponding to a train of kink–antikink nonlinear waves

$$\tilde{D}_j^{n+1} = \tilde{D}_j^n + \Delta\tilde{t} \left(\tilde{D}_h^{(2M)} \tilde{H}_h^{n+\frac{1}{2}} \right)_j, \tag{8.9b}$$

$$\tilde{P}_j^{n+1} = \tilde{P}_j^n + \frac{\Delta\tilde{t}}{2} \left(\tilde{J}_j^{n+1} + \tilde{J}_j^n \right), \tag{8.9c}$$

$$\tilde{J}_j^{n+1} = \tilde{J}_j^n - \frac{\Delta\tilde{t}}{2} \tilde{\omega}_0^2 \left(\tilde{P}_j^{n+1} + \tilde{P}_j^n \right) + \frac{\Delta\tilde{t}}{2} \tilde{\omega}_p^2 \left(\tilde{E}_j^{n+1} + \tilde{E}_j^n \right), \tag{8.9d}$$

$$\tilde{D}_j^{n+1} = \epsilon_\infty \tilde{E}_j^{n+1} + \tilde{P}_j^{n+1} + \tilde{a} \tilde{Y}_j^{n+1}, \tag{8.9e}$$

$$\tilde{Y}_j^{n+1} = \tilde{Y}_j^n + \frac{3}{2} \left((\tilde{E}_j^{n+1})^2 + (\tilde{E}_j^n)^2 \right) \left(\tilde{E}_j^{n+1} - \tilde{E}_j^n \right), \tag{8.9f}$$

for $0 \leq j \leq I - 1$. Assuming that the grid functions $\tilde{E}_h^n, \tilde{P}_h^n, \tilde{J}_h^n$ and $\tilde{H}_h^{n+\frac{1}{2}}$ have been computed, the leap-frog scheme proceeds as follows:

1. **Update of field \tilde{D}_h^{n+1} .**

The field \tilde{D}_h^{n+1} is updated from Eq. (8.9b).

2. **Update of field \tilde{E}_h^{n+1} .**

From (8.9c)-(8.9f), we obtain the following cubic Equation in \tilde{E}_h^{n+1}

$$\begin{aligned} & \frac{3}{2} \tilde{a} (\tilde{E}_j^{n+1})^3 - \frac{3}{2} \tilde{a} \tilde{E}_j^n (\tilde{E}_j^{n+1})^2 + \left[\epsilon_\infty + \frac{3}{2} \tilde{a} (\tilde{E}_j^n)^2 + \frac{\Delta\tilde{t}^2 \tilde{\omega}_p^2}{4K_+} \right] \tilde{E}_j^{n+1} \\ & = \left[\epsilon_\infty - \frac{\Delta\tilde{t}^2 \tilde{\omega}_p^2}{4K_+} + \frac{3}{2} \tilde{a} (\tilde{E}_j^n)^2 \right] \tilde{E}_j^n + \frac{\Delta\tilde{t}^2 \tilde{\omega}_0^2}{2K_+} \tilde{P}_j^n \\ & \quad - \frac{\Delta\tilde{t}}{2} \left(1 + \frac{K_-}{K_+} \right) \tilde{J}_j^n + \left(\tilde{D}_j^{n+1} - \tilde{D}_j^n \right), \end{aligned} \tag{8.10}$$

where $K_- = 1 - \frac{\Delta\tilde{t}^2}{4} \tilde{\omega}_0^2$ and $K_+ = 1 + \frac{\Delta\tilde{t}^2}{4} \tilde{\omega}_0^2$. We update the field \tilde{E}_h^{n+1} by solving (8.10) using Newton’s method with a Cholesky factorization for the coefficient matrix to improve computational speed.

3. **Update of field $\tilde{H}_h^{n+\frac{3}{2}}$.**

The field $\tilde{H}_h^{n+\frac{3}{2}}$ is updated from Eq. (8.9a).

4. **Update of fields \tilde{P}_h^{n+1} and \tilde{J}_h^{n+1} .**

Finally, we update the field \tilde{J}_h^{n+1} and \tilde{P}_h^{n+1} . From (8.9c) and (8.9d), we get

$$\tilde{J}_h^{n+1} = \frac{K_-}{K_+} \tilde{J}_h^n - \frac{\Delta \tilde{t}}{K_+} \tilde{\omega}_0^2 \tilde{P}_h^n + \frac{\Delta \tilde{t}}{2K_+} \tilde{\omega}_p^2 (\tilde{E}_h^{n+1} + \tilde{E}_h^n), \tag{8.11}$$

$$\tilde{P}_h^{n+1} = \left(1 - \frac{\Delta \tilde{t}^2 \tilde{\omega}_0^2}{2K_+}\right) \tilde{P}_h^n + \frac{\Delta \tilde{t}}{2} \left(1 + \frac{K_-}{K_+}\right) \tilde{J}_h^n + \frac{\Delta \tilde{t}^2 \tilde{\omega}_0^2}{4K_+} (\tilde{E}_h^{n+1} + \tilde{E}_h^n). \tag{8.12}$$

8.1.2 Implementation of (2, 2M) Trapezoidal Scheme

Let $M \in \mathbb{N}$. The fully discrete equations for the (2, 2M) FDTD trapezoidal scheme for the dimensionless Maxwell system (8.5)–(8.6) for the travelling wave problem is given as

$$\tilde{H}_{j+\frac{1}{2}}^{n+1} = \tilde{H}_{j+\frac{1}{2}}^n + \frac{\Delta \tilde{t}}{2} \left(\mathcal{D}_h^{(2M)} \tilde{E}_h^{n+1} + \mathcal{D}_h^{(2M)} \tilde{E}_h^n\right)_{j+\frac{1}{2}}, \tag{8.13a}$$

$$\tilde{D}_j^{n+1} = \tilde{D}_j^n + \frac{\Delta \tilde{t}}{2} \left(\tilde{\mathcal{D}}_h^{(2M)} \tilde{H}_h^{n+1} + \tilde{\mathcal{D}}_h^{(2M)} \tilde{H}_h^n\right)_j, \tag{8.13b}$$

$$\tilde{P}_j^{n+1} = \tilde{P}_j^n + \frac{\Delta \tilde{t}}{2} \left(\tilde{J}_j^{n+1} + \tilde{J}_j^n\right), \tag{8.13c}$$

$$\tilde{J}_j^{n+1} = \tilde{J}_j^n - \frac{\Delta \tilde{t}}{2} \tilde{\omega}_0^2 \left(\tilde{P}_j^{n+1} + \tilde{P}_j^n\right) + \frac{\Delta \tilde{t}}{2} \tilde{\omega}_p^2 \left(\tilde{E}_j^{n+1} + \tilde{E}_j^n\right), \tag{8.13d}$$

$$\tilde{D}_j^{n+1} = \epsilon_\infty \tilde{E}_j^{n+1} + \tilde{P}_j^{n+1} + \tilde{a} \tilde{Y}_j^{n+1}, \tag{8.13e}$$

$$\tilde{Y}_j^{n+1} = \tilde{Y}_j^n + \frac{3}{2} \left(\tilde{E}_j^{n+1}\right)^2 + \left(\tilde{E}_j^n\right)^2 \left(\tilde{E}_j^{n+1} - \tilde{E}_j^n\right). \tag{8.13f}$$

Assuming that the grid functions \tilde{E}_h^n , \tilde{P}_h^n , \tilde{J}_h^n , and $\tilde{H}_h^{n+\frac{1}{2}}$ have been computed, the trapezoidal scheme then proceeds as follows:

1. **Update of field \tilde{E}_h^{n+1}**

From (8.13a) and (8.13b), we get

$$\tilde{D}_j^{n+1} - \tilde{D}_j^n = \Delta \tilde{t} \left(\tilde{\mathcal{D}}_h^{(2M)} \tilde{H}_h^n\right)_j + \frac{\Delta \tilde{t}^2}{4} \left(\tilde{\mathcal{D}}_h^{(2M)} \mathcal{D}_h^{(2M)} \tilde{E}_h^{n+1} + \tilde{\mathcal{D}}_h^{(2M)} \mathcal{D}_h^{(2M)} \tilde{E}_h^n\right)_j. \tag{8.14}$$

From Eqs. (8.13c)–(8.13f), we have

$$\begin{aligned} & \frac{3}{2} \tilde{a} (\tilde{E}_j^{n+1})^3 - \frac{3}{2} \tilde{a} \tilde{E}_j^n (\tilde{E}_j^{n+1})^2 + \left[\epsilon_\infty + \frac{3}{2} \tilde{a} (\tilde{E}_j^n)^2 + \frac{\Delta \tilde{t}^2 \tilde{\omega}_p^2}{4K_+} \right] \tilde{E}_j^{n+1} \\ &= \left[\epsilon_\infty - \frac{\Delta \tilde{t}^2 \tilde{\omega}_p^2}{4K_+} + \frac{3}{2} \tilde{a} (\tilde{E}_j^n)^2 \right] \tilde{E}_j^n + \frac{\Delta \tilde{t}^2 \tilde{\omega}_0^2}{2K_+} \tilde{P}_j^n \\ & \quad - \frac{\Delta \tilde{t}}{2} \left(1 + \frac{K_-}{K_+}\right) \tilde{J}_j^n + \left(\tilde{D}_j^{n+1} - \tilde{D}_j^n\right). \end{aligned} \tag{8.15}$$

Solving the system of Eqs. (8.14) and (8.15) simultaneously, we obtain the field \tilde{E}_h^{n+1} .

2. **Update of field \tilde{H}_h^{n+1}**

The field \tilde{H}_h^{n+1} is updated from (8.13a).

3. **Update of field** \tilde{D}_h^{n+1}

The field \tilde{D}_h^{n+1} is updated from (8.13b).

4. **Update of fields** \tilde{P}_h^{n+1} **and** \tilde{J}_h^{n+1}

Finally, we use Eqs. (8.11) and (8.12) to update the fields \tilde{J}_h^{n+1} and \tilde{P}_h^{n+1} .

8.1.3 Results of Numerical Simulations for Kink–Antikink Solutions

We choose the following parameter values (see also [43])

$$\epsilon_\infty = 2.25, \epsilon_s = 5.25, \beta = \epsilon_s - \epsilon_\infty, \tilde{\omega}_0 = 93.627179982222216, \tilde{\omega}_p = \tilde{\omega}_0\sqrt{\beta}, \tag{8.16}$$

$$\tilde{a} = \epsilon_\infty/3, v = 0.6545/\sqrt{\epsilon_\infty}, \tilde{E}(0) = 0, \tilde{W}(0) = 0.24919666777865812. \tag{8.17}$$

The initial conditions to the dimensionless Maxwell’s equations (8.5)–(8.6) are

$$\tilde{E}(\tilde{x}, 0) = \tilde{E}(\tilde{x}), \quad \tilde{H}(\tilde{x}, 0) = -\frac{1}{v}\tilde{E}(\tilde{x}), \quad \tilde{D}(\tilde{x}, 0) = \frac{1}{v^2}\tilde{E}(\tilde{x}), \tag{8.18}$$

$$\tilde{P}(\tilde{x}, 0) = \left(\frac{1}{v^2} - \epsilon_\infty\right)\tilde{E}(\tilde{x}) - \tilde{a}\tilde{E}^3(\tilde{x}), \tag{8.19}$$

$$\tilde{J}(\tilde{x}, 0) = \left(\epsilon_\infty v - \frac{1}{v}\right)\tilde{W}(\tilde{x}) + 3\tilde{a}v\tilde{W}(\tilde{x})\tilde{E}^2(\tilde{x}). \tag{8.20}$$

Let M be 1, 2 or 3. The domain is $[0, L]$ with $L = 6$. A train of kink and anti-kink solutions can be obtained numerically using either the $(2, 2M)$ leap-frog FDTD scheme (8.9) or trapezoidal FDTD method (8.13) initialized by the conditions (8.18)–(8.20). The initial condition $\tilde{E}(x, 0)$ is the solution of the ODE system (8.8) at $\tilde{t} = 0$ solved using an explicit Runge–Kutta (4,5) method. We simulate the $(2, 2M)$ leap-frog and trapezoidal FDTD methods with the initial conditions above and obtain numerical solutions at the time $T = 6/v$, at which the wave travels back to the same position as the initial condition.

We list ℓ^2 and ℓ^∞ errors and orders of spatial accuracy of the electric field \tilde{E} in Table 1 where the ℓ^2 and ℓ^∞ errors between a reference solution, \tilde{E}_{ref} , computed on a very fine mesh, and the numerical solution at the time T , are given by

$$\ell^2\text{errors}(h, T) := \left(\sum_{\ell=0}^{I-1} h|\tilde{E}_{ref,\ell}^N - \tilde{E}_\ell^N|^2\right)^{1/2}, \tag{8.21}$$

$$\ell^\infty\text{errors}(h, T) := \max_{0 \leq \ell \leq I-1} |\tilde{E}_{ref,\ell}^N - \tilde{E}_\ell^N|. \tag{8.22}$$

To obtain these errors we have computed reference solutions with a large number of grid points $I = 7680, 3840$, and 1920 . The time and space steps are chosen as $\Delta\tilde{t} = h$ for the $(2, 2)$ schemes, $\Delta\tilde{t} = \frac{h}{2\kappa}$ for $(2, 4)$ schemes with $\kappa = 1, 2, 4, 8$, and $\Delta\tilde{t} = \frac{h}{2\kappa^2}$ for $(2, 6)$ schemes with $\kappa = 1, 2, 4, 8$, and $h = L/I$. As seen in Table 1, the schemes achieve the expected spatial order of accuracy $2M$ for each of the cases $M = 1, 2, 3$, and the slight order reduction for $M = 3$ can be improved if a larger value I is chosen in the reference solution.

Next we investigate the behavior of the numerical energy for both the leap-frog and trapezoidal FDTD methods. From Theorems 5.3 and 6.1, by neglecting Raman scattering and dissipation in the linear Lorentz model (Recall $\theta = 0$ and $1/\tilde{\tau} = 0$), we see that both the $(2, 2M)$ leap-frog and trapezoidal FDTD schemes preserve the discrete energy, i.e. the

Table 1 ℓ^2 and ℓ^∞ errors and orders of accuracy for E for the traveling kink and antikink solutions

I	Leap-frog FDTD scheme			Trapezoidal FDTD scheme		
	ℓ^2 errors	Order	ℓ^∞ errors	ℓ^2 errors	Order	ℓ^∞ errors
(2,2)-scheme	30	2.55322e-02	-	2.31248e-02	-	2.94804e-02
	60	1.00514e-02	1.35	1.20993e-02	0.94	1.53088e-02
	120	2.93102e-03	1.78	4.24230e-03	1.51	6.13541e-03
	240	7.32310e-04	2.00	1.17352e-03	1.85	1.88672e-03
	480	1.79228e-04	2.03	2.96233e-04	1.99	4.97048e-04
(2,4)-scheme	30	8.20010e-03	-	5.48738e-03	-	8.50511e-03
	60	1.44661e-03	2.50	1.62087e-03	1.76	1.98204e-03
	120	1.24038e-04	3.54	1.85339e-04	3.13	2.33376e-04
	240	7.98312e-06	3.96	1.38259e-05	3.75	1.68761e-05
	30	4.09488e-03	-	3.47814e-03	-	5.96232e-03
(2,6)-scheme	60	4.30703e-04	3.25	4.45523e-04	2.97	5.46565e-04
	120	1.27974e-05	5.07	1.96577e-05	4.50	2.27924e-05
	240	2.88157e-07	5.47	4.47722e-07	5.46	4.37055e-07
	30	3.02665e-02	-	3.02665e-02	-	2.94804e-02
	60	1.36431e-02	1.15	1.36431e-02	1.15	1.53088e-02
120	4.53999e-03	1.59	4.53999e-03	1.59	6.13541e-03	
240	1.21563e-03	1.90	1.21563e-03	1.90	1.88672e-03	
480	3.03555e-04	2.00	3.03555e-04	2.00	4.97048e-04	
30	1.15914e-02	-	1.15914e-02	-	8.50511e-03	
60	1.81041e-03	2.68	1.81041e-03	2.68	1.98204e-03	
120	1.50179e-04	3.52	1.50179e-04	3.52	2.33376e-04	
240	9.50860e-06	3.98	9.50860e-06	3.98	1.68761e-05	
30	7.52404e-03	-	7.52404e-03	-	5.96232e-03	
60	5.09006e-04	3.89	5.09006e-04	3.89	5.46565e-04	
120	1.38603e-05	5.20	1.38603e-05	5.20	2.27924e-05	
240	2.33965e-07	5.89	2.33965e-07	5.89	4.37055e-07	

schemes conserve discrete energy. Let $0 \leq n \leq N$. The discrete energy satisfies

$$\tilde{\mathcal{E}}_{h,V}^{n+1} = \tilde{\mathcal{E}}_{h,V}^n, \quad \forall n, V = LF \text{ or } V = \text{Trap} \tag{8.23}$$

where the discrete energy for $(2, 2M)$ leap-frog FDTD scheme (8.9) is defined to be

$$\tilde{\mathcal{E}}_{h,LF}^n := \frac{1}{2} \left(\langle \tilde{H}^{n-\frac{1}{2}}, \tilde{H}^{n+\frac{1}{2}} \rangle_{\frac{1}{2},h} + \epsilon_\infty \|\tilde{E}^n\|_{0,h}^2 + \frac{3a}{2} \|(\tilde{E}^n)^2\|_{0,h}^2 + \frac{\omega_0^2}{\omega_p^2} \|\tilde{P}^n\|_{0,h}^2 + \frac{1}{\omega_p^2} \|\tilde{J}^n\|_{0,h}^2 \right). \tag{8.24}$$

The discrete energy for the $(2, 2M)$ trapezoidal FDTD scheme (8.13) is defined to be

$$\tilde{\mathcal{E}}_{h,\text{Trap}}^n := \frac{1}{2} \left(\|\tilde{H}^n\|_{0,h}^2 + \epsilon_\infty \|\tilde{E}^n\|_{0,h}^2 + \frac{3a}{2} \|(\tilde{E}^n)^2\|_{0,h}^2 + \frac{\omega_0^2}{\omega_p^2} \|\tilde{P}^n\|_{0,h}^2 + \frac{1}{\omega_p^2} \|\tilde{J}^n\|_{0,h}^2 \right). \tag{8.25}$$

The behavior of the numerical energy is presented in Fig. 2. To obtain these plots we have used

$$\Delta \tilde{x} = 0.2, \quad \text{and} \quad \Delta \tilde{t} = 0.1.$$

From Fig. 2 we see that the difference of the discrete energy at times \tilde{t}^{n+1} and \tilde{t}^n (see (8.23)) is close to machine epsilon 10^{-16} for both schemes. This agrees with our analysis in Theorem 5.3 for the $(2, 2M)$ leap-frog FDTD schemes and Theorem 6.1 for the trapezoidal FDTD schemes which indicate that both methods conserve their respective discrete energy.

8.2 Soliton Propagation

In this section, we present a second numerical simulation to illustrate soliton propagation modeled by the dimensionless nonlinear Maxwell’s equation on a finite domain [16]. Our simulations will illustrate properties of the $(2, 2M)$ leap-frog and trapezoidal FDTD schemes based on the non-dimensionalized nonlinear Maxwell system (8.5)–(8.6).

We let all given fields be zero at time $\tilde{t} = 0$. At the left grid boundary we use the following source condition for the electric field,

$$\tilde{E}(\tilde{x} = 0, \tilde{t}) = f(\tilde{t}) \cos(\Omega_0 \tilde{t}), \quad t \geq 0 \tag{8.26}$$

where $f(\tilde{t}) = \zeta \operatorname{sech}(\tilde{t} - 20)$. We simulate the transient fundamental ($\zeta = 1$) and second-order ($\zeta = 2$) temporal soliton evolution. As shown in [16], the left boundary condition for the magnetic field can be obtained from Maxwell’s equations and the inverse Fourier transform of H as

$$\tilde{H}(\tilde{x} = 0, \tilde{t}) \simeq \frac{1}{2} \left[\frac{1}{Z} f(\tilde{t}) - i \left(\frac{1}{Z} \right)' f'(\tilde{t}) - \frac{1}{2} \left(\frac{1}{Z} \right)'' f''(\tilde{t}) \right] e^{i\Omega_0 \tilde{t}} + c.c., \tag{8.27}$$

where, Z and all its derivatives with respect to ω are derived from the condition $Z(\omega) = -\omega/k$ at $\omega = \Omega_0$, and $c.c.$ denotes the complex conjugate of the first term,

At the right boundary we assume an absorbing boundary condition of the form

$$\left(\frac{\partial}{\partial \tilde{t}} \tilde{E}^{n+\frac{1}{2}} \right)_{I-\frac{1}{2}} = -\frac{1}{\sqrt{\epsilon_\infty}} \left(\frac{\partial}{\partial \tilde{x}} \tilde{E}^{n+\frac{1}{2}} \right)_{I-\frac{1}{2}}, \tag{8.28}$$

which we discretize using a centered difference scheme as

$$\frac{1}{\Delta \tilde{t}} \left(\tilde{E}_{I-\frac{1}{2}}^{n+\frac{1}{2}} - \tilde{E}_{I-\frac{1}{2}}^n \right) = -\frac{1}{\sqrt{\epsilon_\infty}} \frac{1}{\Delta \tilde{x}} \left(\tilde{E}_I^{n+\frac{1}{2}} - \tilde{E}_{I-1}^{n+\frac{1}{2}} \right). \tag{8.29}$$

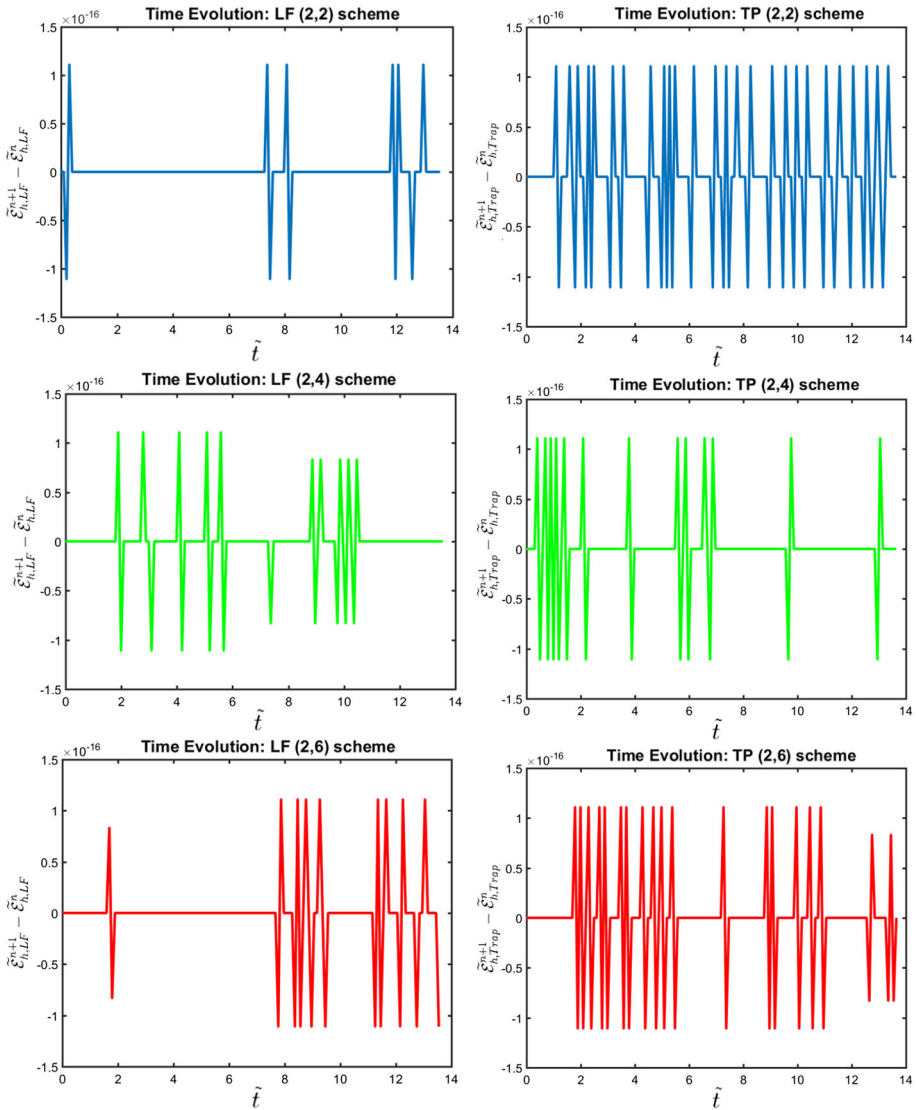


Fig. 2 Discrete energy conservation: $(2, 2M)$ leap-frog FDTD schemes and trapezoidal FDTD schemes for $M = 1, 2, 3$. First column: the leap-frog FDTD schemes; second column: the trapezoidal FDTD schemes. First row: schemes of order $(2,2)$; second row: schemes of order $(2,4)$; third row: schemes of order $(2,6)$

Since the electric field is not defined on the dual spatial grid, we don't have information about the electric field at the node $I - \frac{1}{2}$. Thus we approximate the values of the electric field at $I - \frac{1}{2}$ by the average of the electric field at grid points I and $I - 1$. Similarly we do not have information about the electric field values at $\tilde{t}^{n+\frac{1}{2}}$. Thus we approximate the value of the electric field at this point by its average at the time \tilde{t}^n and \tilde{t}^{n+1} . Using averaged approximations and simplifying, we get the following discretized absorbing boundary condition that is imposed on the right boundary of the domain, Ω ,

$$\tilde{E}_I^{n+1} = \tilde{E}_{I-1}^n + \frac{1-\nu}{1+\nu} \left(\tilde{E}_I^n - \tilde{E}_{I-1}^{n+1} \right). \tag{8.30}$$

where $\nu := \frac{1}{\sqrt{\epsilon_\infty}} \frac{\Delta \tilde{t}}{\Delta \tilde{x}}$.

We present simulations of the propagation of solitons using the (2, 2) and (2, 4) schemes. In the (2, 4) schemes we need to discretize the spatial derivatives at the boundary using one sided derivatives. We use the one sided approximations derived in [51] that are atleast fourth order accurate to maintain the fourth order spatial accuracy of the schemes. For an unknown field U , these are given as

$$\frac{\partial U}{\partial x} \Big|_{\frac{1}{2}} = \frac{1}{24\Delta x} (-22U_0 + 17U_1 + 9U_2 - 5U_3 + U_4), \tag{8.31}$$

$$\frac{\partial U}{\partial x} \Big|_1 = \frac{1}{24\Delta x} \left(-23U_{\frac{1}{2}} + 21U_{\frac{3}{2}} + 3U_{\frac{5}{2}} - U_{\frac{7}{2}} \right), \tag{8.32}$$

$$\frac{\partial U}{\partial x} \Big|_{I-1} = \frac{1}{24\Delta x} \left(23U_{I-\frac{1}{2}} - 21U_{I-\frac{3}{2}} - 3U_{I-\frac{5}{2}} + U_{I-\frac{7}{2}} \right), \tag{8.33}$$

$$\frac{\partial U}{\partial x} \Big|_{I-\frac{1}{2}} = \frac{1}{24\Delta x} (22U_I - 17U_{I-1} - 9U_{I-2} + 5U_{I-3} - U_{I-4}). \tag{8.34}$$

For $M > 3$, appropriate $2M$ th order one-sided approximations will be needed to be defined at the boundary in order to maintain the overall $2M$ accuracy in space. Since, developing boundary conditions is not the main goal of this paper, we leave this construction to future work, and only consider the case $M = 1, 2$ here.

8.2.1 Implementation of (2, 2M) FDTD Leap-Frog Scheme

In this section we discuss the implementation of the (2, 2M) leap-frog FDTD scheme, for $M = 1, 2$, given in system (5.1) below.

The (2, 2M) leap-frog FDTD schemes for (8.5)–(8.6), i.e. the analogues of Eq. (5.1) are given as follows. Let $0 \leq j \leq I - 1$. We have the system

$$\tilde{H}_{j+\frac{1}{2}}^{n+\frac{1}{2}} = \tilde{H}_{j+\frac{1}{2}}^{n-\frac{1}{2}} + \Delta \tilde{t} \left(\mathcal{D}_h^{(2M)} \tilde{E}_h^n \right)_{j+\frac{1}{2}}, \tag{8.35a}$$

$$\tilde{D}_j^{n+1} = \tilde{D}_j^n + \Delta \tilde{t} \left(\tilde{\mathcal{D}}_h^{(2M)} \tilde{H}_h^{n+\frac{1}{2}} \right)_j, \tag{8.35b}$$

$$\tilde{P}_j^{n+1} = \tilde{P}_j^n + \frac{\Delta \tilde{t}}{2} \left(\tilde{J}_j^{n+1} + \tilde{J}_j^n \right), \tag{8.35c}$$

$$\tilde{J}_j^{n+1} = \tilde{J}_j^n - \frac{\Delta \tilde{t}}{2\tilde{\tau}} \left(\tilde{J}_j^{n+1} + \tilde{J}_j^n \right) - \frac{\Delta \tilde{t}}{2} \tilde{\omega}_0^2 \left(\tilde{P}_j^{n+1} + \tilde{P}_j^n \right) + \frac{\Delta \tilde{t}}{2} \tilde{\omega}_p^2 \left(\tilde{E}_j^{n+1} + \tilde{E}_j^n \right), \tag{8.35d}$$

$$\tilde{Q}_j^{n+1} = \tilde{Q}_j^n + \frac{\Delta \tilde{t}}{2} \left(\tilde{\sigma}_j^{n+1} + \tilde{\sigma}_j^n \right), \tag{8.35e}$$

$$\tilde{\sigma}_j^{n+1} = \tilde{\sigma}_j^n - \frac{\Delta \tilde{t}}{2\tilde{\tau}_v} \left(\tilde{\sigma}_j^{n+1} + \tilde{\sigma}_j^n \right) - \frac{\Delta \tilde{t}}{2} \tilde{\omega}_v^2 \left(\tilde{Q}_j^{n+1} + \tilde{Q}_j^n \right) + \Delta \tilde{t} \tilde{\omega}_v^2 \tilde{E}_j^n \tilde{E}_j^{n+1}, \tag{8.35f}$$

$$\tilde{D}_j^{n+1} = \epsilon_\infty \tilde{E}_j^{n+1} + \tilde{P}_j^{n+1} + \tilde{a}(1-\theta) \tilde{Y}_j^{n+1} + \tilde{a}\theta \tilde{Q}_j^{n+1} \tilde{E}_j^{n+1}, \tag{8.35g}$$

$$\tilde{Y}_j^{n+1} = \tilde{Y}_j^n + \frac{3}{2} \left((\tilde{E}_j^{n+1})^2 + (\tilde{E}_j^n)^2 \right) \left(\tilde{E}_j^{n+1} - \tilde{E}_j^n \right). \tag{8.35h}$$

Assuming that the grid functions $\tilde{E}_h^n, \tilde{P}_h^n, \tilde{J}_h^n, \tilde{Q}_h^n, \tilde{\sigma}_h^n$ and $\tilde{H}_h^{n+\frac{1}{2}}$ have been computed, the leap-frog FDTD scheme then proceeds as follows:

1. **Update of field \tilde{D}_h^{n+1}**

First, we update the field values \tilde{D}_h^{n+1} from (8.35b).

2. **Update of field \tilde{E}_h^{n+1}**

From (8.35b)-(8.35d) and (8.35g)-(8.35h), we obtain the following systems

$$\begin{aligned} & \frac{3}{2}\tilde{a}(1-\theta)(\tilde{E}_j^{n+1})^3 - \frac{3}{2}\tilde{a}(1-\theta)\tilde{E}_j^n(\tilde{E}_j^{n+1})^2 \\ & + \left[\epsilon_\infty + \frac{3}{2}\tilde{a}(1-\theta)(\tilde{E}_j^n)^2 + \frac{\Delta\tilde{t}^2\tilde{\omega}_p^2}{4K_+} \right] \tilde{E}_j^{n+1} + a\theta \left(\tilde{Q}_j^{n+1}\tilde{E}_j^{n+1} - \tilde{Q}_j^n\tilde{E}_j^n \right) \\ & = \left[\frac{\epsilon_\infty - \Delta\tilde{t}^2\tilde{\omega}_p^2}{4K_+} + \frac{3}{2}\tilde{a}(1-\theta)(\tilde{E}_j^n)^2 \right] \tilde{E}_j^n \\ & + \frac{\Delta\tilde{t}^2\tilde{\omega}_0^2}{2K_+}\tilde{P}_j^n - \frac{\Delta\tilde{t}}{2} \left(1 + \frac{K_-}{K_+} \right) \tilde{J}_j^n - \left(\tilde{D}_j^{n+1} - \tilde{D}_j^n \right) \end{aligned} \tag{8.36}$$

where

$$K_- = 1 - \frac{\Delta\tilde{t}}{2\tilde{\tau}} - \frac{\Delta\tilde{t}^2}{4}\tilde{\omega}_0^2 \quad \text{and} \quad K_+ = 1 + \frac{\Delta\tilde{t}}{2\tilde{\tau}} + \frac{\Delta\tilde{t}^2}{4}\tilde{\omega}_0^2.$$

Moreover using (8.35e) and (8.35f), we get

$$\tilde{Q}_j^{n+1}\tilde{E}_j^{n+1} = \frac{\Delta\tilde{t}^2\tilde{\omega}_v^2}{2K_+^*}\tilde{E}_j^n(\tilde{E}_j^{n+1})^2 + \left[\left(1 - \frac{\tilde{\omega}_v^2\Delta\tilde{t}^2}{2K_+^*} \right) \tilde{Q}_j^n + \frac{\Delta\tilde{t}}{2} \left(1 + \frac{K_-^*}{K_+^*} \right) \tilde{\sigma}_j^n \right] \tilde{E}_j^{n+1}, \tag{8.37}$$

where

$$K_-^* = 1 - \frac{\Delta\tilde{t}}{2\tilde{\tau}_v} - \frac{\Delta\tilde{t}^2}{4}\tilde{\omega}_v^2 \quad \text{and} \quad K_+^* = 1 + \frac{\Delta\tilde{t}}{2\tilde{\tau}_v} + \frac{\Delta\tilde{t}^2}{4}\tilde{\omega}_v^2.$$

We update the interior grid values of the field \tilde{E}_j^{n+1} for $j = 1, \dots, I - 1$ by solving the systems of Eqs. (8.36) and (8.37). The left boundary grid value of the field \tilde{E}_h is updated by (8.26), and the absorbing boundary condition (8.30) is applied to update the right boundary grid value of the field \tilde{E}_h .

3. **Update of field $\tilde{H}_h^{n+\frac{3}{2}}$**

To update the field $\tilde{H}_h^{n+\frac{3}{2}}$ we use (8.35a), with $n = n + 1$.

We update the left boundary grid value $\tilde{H}_1^{n+\frac{3}{2}}$ by using the boundary conditions derived from (8.27).

4. **Update of fields \tilde{J}_h^{n+1} and \tilde{P}_h^{n+1}**

We update the field \tilde{J}_h^{n+1} and \tilde{P}_h^{n+1} from (8.35c) and (8.35d), respectively.

5. **Update of fields \tilde{Q}_h^{n+1} and $\tilde{\sigma}_h^{n+1}$**

Finally, we update the field $\tilde{\sigma}_h^{n+1}$ and \tilde{Q}_h^{n+1} . From (8.35e) and (8.35f), we get

$$\tilde{\sigma}_j^{n+1} = \frac{K^*}{K_+^*} \tilde{\sigma}_j^n - \frac{\Delta \tilde{t}}{K_+^*} \tilde{\omega}_v^2 \tilde{Q}_j^n + \frac{\Delta \tilde{t}}{K_+^*} \tilde{\omega}_v^2 \tilde{E}_j^{n+1} \tilde{E}_j^n, \tag{8.38}$$

$$\tilde{Q}_j^{n+1} = \left(1 - \frac{\Delta \tilde{t}^2 \tilde{\omega}_v^2}{2K_+^*}\right) \tilde{Q}_j^n + \frac{\Delta \tilde{t}}{2} \left(1 + \frac{K^*}{K_+^*}\right) \tilde{\sigma}_j^n + \frac{\Delta \tilde{t}^2 \tilde{\omega}_v^2}{2K_+^*} \tilde{E}_j^{n+1} \tilde{E}_j^n. \tag{8.39}$$

When $M = 2$, we use the one side approximations (8.31)–(8.34) to update the grid values of the fields \tilde{D}_h^{n+1} and \tilde{H}_h^{n+1} near domain boundaries.

8.2.2 Implementation of (2, 2M) Trapezoidal FDTD Scheme

In this section we discuss the implementation of the (2, 2M) trapezoidal scheme given in system (6.1) below.

The (2, 2M) trapezoidal FDTD schemes for the non-dimensionalized nonlinear Maxwell system (8.5)–(8.6), i.e. the analogues of Eq. (6.1), are given as follows. Let $0 \leq j \leq I - 1$

$$\tilde{H}_{j+\frac{1}{2}}^{n+1} = \tilde{H}_{j+\frac{1}{2}}^n + \frac{\Delta \tilde{t}}{2} \left(\mathcal{D}_h^{(2M)} \tilde{E}_h^{n+1} + \mathcal{D}_h^{(2M)} \tilde{E}_h^n \right)_{j+\frac{1}{2}}, \tag{8.40a}$$

$$\tilde{D}_j^{n+1} = \tilde{D}_j^n + \frac{\Delta \tilde{t}}{2} \left(\tilde{\mathcal{D}}_h^{(2M)} \tilde{H}_h^{n+1} + \tilde{\mathcal{D}}_h^{(2M)} \tilde{H}_h^n \right)_j, \tag{8.40b}$$

$$\tilde{P}_j^{n+1} = \tilde{P}_j^n + \frac{\Delta \tilde{t}}{2} \left(\tilde{J}_j^{n+1} + \tilde{J}_j^n \right), \tag{8.40c}$$

$$\tilde{J}_j^{n+1} = \tilde{J}_j^n - \frac{\Delta \tilde{t}}{2\tau} \left(\tilde{J}_j^{n+1} + \tilde{J}_j^n \right) - \frac{\Delta \tilde{t}}{2} \tilde{\omega}_0^2 \left(\tilde{P}_j^{n+1} + \tilde{P}_j^n \right) + \frac{\Delta \tilde{t}}{2} \tilde{\omega}_p^2 \left(\tilde{E}_j^{n+1} + \tilde{E}_j^n \right), \tag{8.40d}$$

$$\tilde{Q}_j^{n+1} = \tilde{Q}_j^n + \frac{\Delta \tilde{t}}{2} \left(\tilde{\sigma}_j^{n+1} + \tilde{\sigma}_j^n \right), \tag{8.40e}$$

$$\tilde{\sigma}_j^{n+1} = \tilde{\sigma}_j^n - \frac{\Delta \tilde{t}}{2\tau_v} \left(\tilde{\sigma}_j^{n+1} + \tilde{\sigma}_j^n \right) - \frac{\Delta \tilde{t}}{2} \tilde{\omega}_v^2 \left(\tilde{Q}_j^{n+1} + \tilde{Q}_j^n \right) + \Delta \tilde{t} \tilde{\omega}_v^2 \tilde{E}_j^n \tilde{E}_j^{n+1}, \tag{8.40f}$$

$$\tilde{D}_j^{n+1} = \epsilon_\infty \tilde{E}_j^{n+1} + \tilde{P}_j^{n+1} + \tilde{a}(1 - \theta) \tilde{Y}_j^{n+1} + \tilde{a}\theta \tilde{Q}_j^{n+1} \tilde{E}_j^{n+1}, \tag{8.40g}$$

$$\tilde{Y}_j^{n+1} = \tilde{Y}_j^n + \frac{3}{2} \left((\tilde{E}_j^{n+1})^2 + (\tilde{E}_j^n)^2 \right) \left(\tilde{E}_j^{n+1} - \tilde{E}_j^n \right). \tag{8.40h}$$

Assuming for $M = 1, 2$, that the grid functions $\tilde{E}_h^n, \tilde{P}_h^n, \tilde{J}_h^n, \tilde{Q}_h^n, \tilde{\sigma}_h^n, \tilde{H}_h^n$, have been computed, the trapezoidal scheme then proceeds as follows:

- Update of field \tilde{E}_h^{n+1}** From (8.40a) and (8.40b), we have

$$\tilde{D}_j^{n+1} - \tilde{D}_j^n = \Delta \tilde{t} \left(\tilde{\mathcal{D}}_h^{(2M)} \tilde{H}_h^n \right)_j + \frac{\Delta \tilde{t}^2}{4} \left(\tilde{\mathcal{D}}_h^{(2M)} \mathcal{D}_h^{(2M)} \tilde{E}_h^{n+1} + \tilde{\mathcal{D}}_h^{(2M)} \mathcal{D}_h^{(2M)} \tilde{E}_h^n \right)_j. \tag{8.41}$$

From Eqs. (8.40c)–(8.40d) and (8.40g)–(8.40h), we obtain

$$\begin{aligned} \tilde{D}_j^{n+1} - \tilde{D}_j^n &= \frac{3}{2} \tilde{a}(1 - \theta) (\tilde{E}_j^{n+1})^3 - \frac{3}{2} \tilde{a}(1 - \theta) \tilde{E}_j^n (\tilde{E}_j^{n+1})^2 \\ &+ \left[\epsilon_\infty + \frac{3}{2} \tilde{a}(1 - \theta) (\tilde{E}_j^n)^2 + \frac{\Delta \tilde{t}^2 \tilde{\omega}_p^2}{4K_+} \right] \tilde{E}_j^{n+1} \end{aligned}$$

$$\begin{aligned}
 & + \left[\frac{\Delta \tilde{t}^2 \tilde{\omega}_p^2}{4K_+} - \epsilon_\infty - \frac{3}{2} \tilde{a}(1 - \theta)(\tilde{E}_j^n)^2 \right] \tilde{E}_j^n - \frac{\Delta \tilde{t}^2 \tilde{\omega}_0^2}{2K_+} \tilde{P}_j^n + \frac{\Delta \tilde{t}}{2} \left(1 + \frac{K_-}{K_+} \right) \tilde{J}_j^n \\
 & + a\theta \left(\tilde{Q}_j^{n+1} \tilde{E}_j^{n+1} - \tilde{Q}_j^n \tilde{E}_j^n \right), \tag{8.42}
 \end{aligned}$$

where $\tilde{Q}_j^{n+1} \tilde{E}_j^{n+1}$ in the Eq. (8.42) satisfies Eq. (8.37). Solving the systems (8.41), (8.42) and (8.37) for $j = 1, \dots, I - 1$, we obtain \tilde{E}_j^{n+1} at the interior grid points. The left boundary grid values of the field \tilde{E}_h is updated by (8.26), and the absorbing boundary condition (8.30) is applied to update the right boundary grid value of the field \tilde{E}_h .

2. **Update of field \tilde{H}_h^{n+1}** From (8.40a), we get

$$\tilde{H}_{j+\frac{1}{2}}^{n+1} = \tilde{H}_{j+\frac{1}{2}}^n + \frac{\Delta \tilde{t}}{2} \left(\mathcal{D}_h^{(2M)} \tilde{E}_h^{n+1} + \mathcal{D}_h^{(2M)} \tilde{E}_h^n \right)_{j+\frac{1}{2}}. \tag{8.43}$$

We update the left boundary grid value $\tilde{H}_{\frac{1}{2}}^{n+1}$ by using the boundary conditions derived from (8.27). When $M = 2$, we use the one side approximations (8.31)-(8.34) to update the first and last few grid values of \tilde{H}_h^n on the boundary of Ω . As in the leap-frog case, we do not consider the case $M > 2$ here.

3. **Update of field \tilde{D}_h^{n+1}** From (8.13b), we solve for \tilde{D}_h^{n+1} in

$$\tilde{D}_j^{n+1} = \tilde{D}_j^n + \frac{\Delta \tilde{t}}{2} \left(\tilde{\mathcal{D}}_h^{(2M)} \tilde{H}_h^{n+1} + \tilde{\mathcal{D}}_h^{(2M)} \tilde{H}_h^n \right)_j. \tag{8.44}$$

When $M = 2$, we use the one side approximations (8.31)-(8.34) to update the first and last few grid values of the field \tilde{D}_h^{n+1} on the boundary of Ω .

4. **Update of fields \tilde{J}_h^{n+1} and \tilde{P}_h^{n+1}**

We use Eqs. (8.11) and (8.12) to update the fields \tilde{J}_h^{n+1} and \tilde{P}_h^{n+1} .

5. **Update of fields \tilde{Q}_h^{n+1} and $\tilde{\sigma}_h^{n+1}$**

Finally, we update the field $\tilde{\sigma}_h^{n+1}$ and \tilde{Q}_h^{n+1} . From (8.40e) and (8.40f), we get

$$\tilde{\sigma}_j^{n+1} = \frac{K_-^*}{K_+^*} \tilde{\sigma}_j^n - \frac{\Delta \tilde{t}}{K_+^*} \tilde{\omega}_v^2 \tilde{Q}_j^n + \frac{\Delta \tilde{t}}{K_+^*} \tilde{\omega}_v^2 \tilde{E}_j^{n+1} \tilde{E}_j^n, \tag{8.45}$$

$$\tilde{Q}_j^{n+1} = \left(1 - \frac{\Delta \tilde{t}^2 \tilde{\omega}_v^2}{2K_+^*} \right) \tilde{Q}_j^n + \frac{\Delta \tilde{t}}{2} \left(1 + \frac{K_-^*}{K_+^*} \right) \tilde{\sigma}_j^n + \frac{\Delta \tilde{t}^2 \tilde{\omega}_v^2}{2K_+^*} \tilde{E}_j^{n+1} \tilde{E}_j^n. \tag{8.46}$$

8.2.3 Numerical Results for First and Second Order Soliton Propagation

The parameters in this section are chosen as

$$\begin{aligned}
 \epsilon_\infty &= 2.25, & \epsilon_s &= 5.25, & \beta &= \epsilon_s - \epsilon_\infty, \\
 \tilde{\omega}_0 &= 5.84, & \tilde{\omega}_p &= \tilde{\omega}_0 \sqrt{\beta}, & \tilde{\omega}_v &= 1.28, \\
 \theta &= 0.3, & \tilde{a} &= 0.07, & \Omega_0 &= 12.57, \\
 1/\tilde{\tau} &= 1.168 \times 10^{-5}, & 1/\tilde{\tau}_v &= 29.2/32.
 \end{aligned}$$

We consider soliton propagation on the domain $[0, L]$ with $L = 6$, the uniform spatial step $\Delta \tilde{x} = 0.0047$ corresponding to $I = 7680$, and the time step is chosen as

$$\Delta \tilde{t} = 0.1 \times \Delta \tilde{x}.$$

We simulate the transient fundamental ($\zeta = 1$) and second-order ($\zeta = 2$) temporal soliton evolution using $(2, 2M)$ leap-frog scheme and $(2, 2M)$ trapezoidal scheme for $M = 1, 2$.

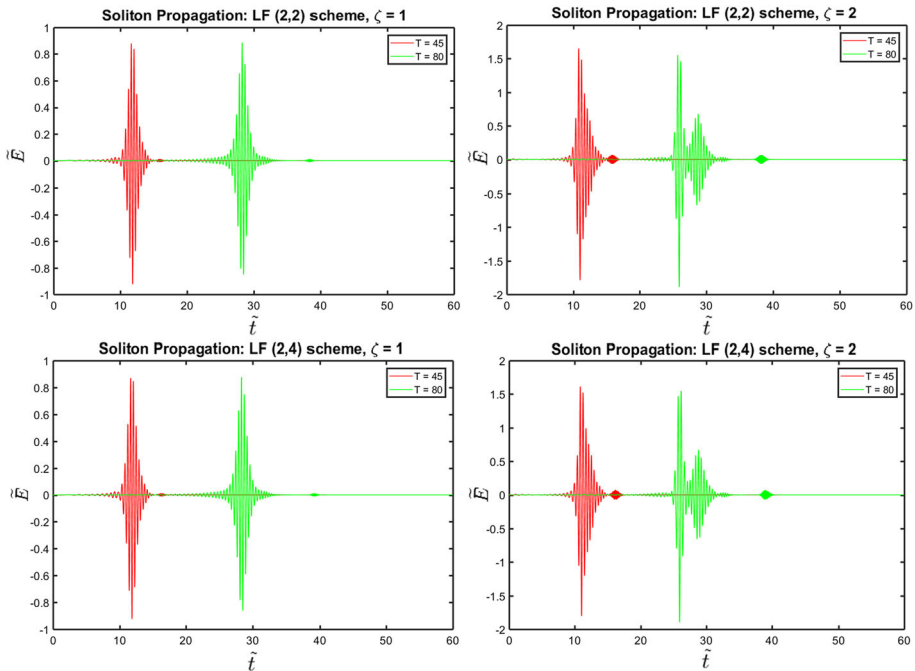


Fig. 3 Soliton propagation: first column: $\zeta = 1$; second column: $\zeta = 2$. First row: the leap-frog (2,2) FDTD scheme; second row: the leap-frog (2,4) FDTD scheme

We present the electric field at time $\tilde{t} = 45$ and 80 in Figs. 3 and 4. The phenomenon of third-harmonic generation results in the separation of the daughter pulse from the main pulse. The daughter pulse separating from the soliton propagates ahead of its main pulse with a peak velocity much shorter than the soliton pulse. Moreover, simulations obtained by employing the leap-frog FDTD scheme and trapezoidal FDTD scheme appear very similar for both the cases $\zeta = 1$ and 2 , as seen in Figs. 3, 4, 5, and 6.

In Figs. 5 and 6, we plot the discrete energy of soliton propagation and the pulse area of the soliton (defined below) with the $(2, 2M)$ leap-frog FDTD and trapezoidal FDTD schemes for $M = 1, 2$. The discrete energy of the leap-frog FDTD scheme and trapezoidal FDTD scheme are defined in (8.24) and (8.25), respectively. From Fig. 5, we see that the discrete energy of both schemes satisfies energy decay after $\tilde{t} = 20$, which is the time when the traveling wave enters the domain. These results agree with the stability properties of leap-frog and trapezoidal FDTD schemes, sd stated in Theorems 5.3 and 6.1, respectively.

The pulse area of the soliton is defined to be the area under the electric field curve over the domain of grid points on which the electric field has values $|\tilde{E}_h| \geq 0.1$. In Fig. 6, the pulse area of the soliton is plotted by using the composite trapezoidal rule. The main purpose of computing the numerical pulse area is to differentiate the velocity peaks of the daughter pulse from the soliton over the domain $|\tilde{E}_h| \geq 0.1$.

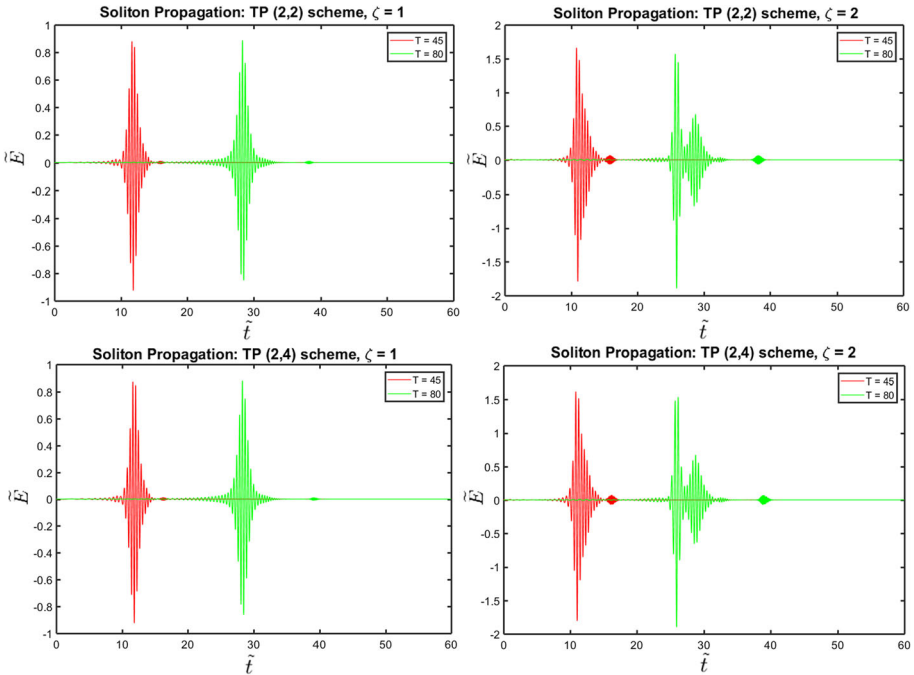


Fig. 4 Soliton propagation: first column: $\zeta = 1$; second column: $\zeta = 2$. First row: the trapezoidal (2,2) FDTD scheme; second row: the trapezoidal (2,4) FDTD scheme

9 Conclusions and Future Directions

In this paper, we developed new high spatial order $(2, 2M)$ FDTD methods with $M \in \mathbb{N}$ that are energy stable and are second order accurate in time for a nonlinear Maxwell model in one spatial dimension. Two types of second order time integrators are used for the time discretization of the nonlinear Maxwell model; the leap-frog and trapezoidal time integrators. The nonlinear Maxwell model includes an instantaneous cubic Kerr nonlinearity as well as both linear and nonlinear Lorentz dispersion, where the nonlinear Lorentz dispersion arises due to Raman scattering. On uniform meshes, the fully discrete FDTD methods are energy stable and we have computed theoretically the Courant stability limits for arbitrary spatial orders for the leap-frog FDTD schemes. The trapezoidal FDTD methods are shown to be unconditionally stable using an energy analysis. The second order temporal accuracy of the methods is obeyed by new time discretizations for the nonlinear terms in the model to provide fully discrete energy identities that respect the energy identities on the continuous level. Numerical simulations are presented for (2,2), (2,4) and (2,6) order methods in the case of periodic boundary conditions and for (2,2) and (2,4) order methods in the case of soliton propagation where absorbing boundary conditions are used. For general boundary conditions, the high order spatial discretizations have to be modified at the boundaries using one sided derivatives. We have done this for the (2,4) order method using results from the literature. For the general $(2, 2M)$ methods with $M \geq 3$, such modified treatments do not seem to be available. We will explore discretizations of general boundary conditions in a future paper.

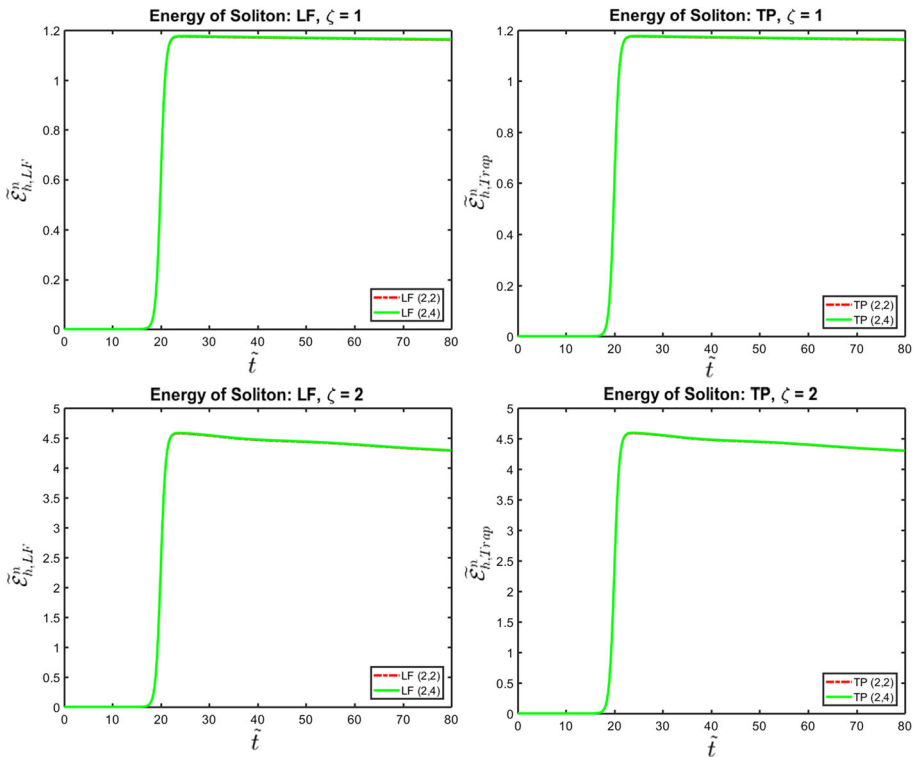


Fig. 5 Numerical energy of transient fundamental ($\zeta = 1$, first row) and second order ($\zeta = 2$, second row) soliton propagation. First column: leap-frog FDTD scheme. Second column: trapezoidal FDTD scheme

We have also presented the extension of the fully discrete leap-frog and trapezoidal FDTD schemes for $M = 1$ to nonuniform grids. We prove that our second order extensions on nonuniform meshes are also energy stable with modified stability conditions for the leap-frog FDTD method, while the trapezoidal FDTD method on nonuniform meshes is unconditionally stable. For the case $M > 1$, the extensions of our schemes to nonuniform meshes are nontrivial, and will be investigated in our future work. Another extension we will explore in the future is the construction of higher order energy stable time stepping schemes.

The analysis of energy relations in one spatial dimension in the nonlinear Maxwell model, as well as the corresponding fully energy stable discretizations presented in this paper provide us insights for the study of higher dimensional cases. We are currently working on extending our energy analysis and numerical methods to two and three dimensional spatial models. In higher spatial dimensions additional properties of the nonlinear Maxwell model have to be taken into account. In particular, the divergence laws are now coupled to the model. In addition, perfectly matched layer (PML) models will need to be constructed to handle absorbing boundary conditions. We will be exploring all these aspects in future work. We are also currently studying the dispersion errors of the $(2, 2M)$ schemes constructed in this paper, and comparison will be made between these and other available numerical solvers such as the discontinuous Galerkin methods constructed in our recent work [5].

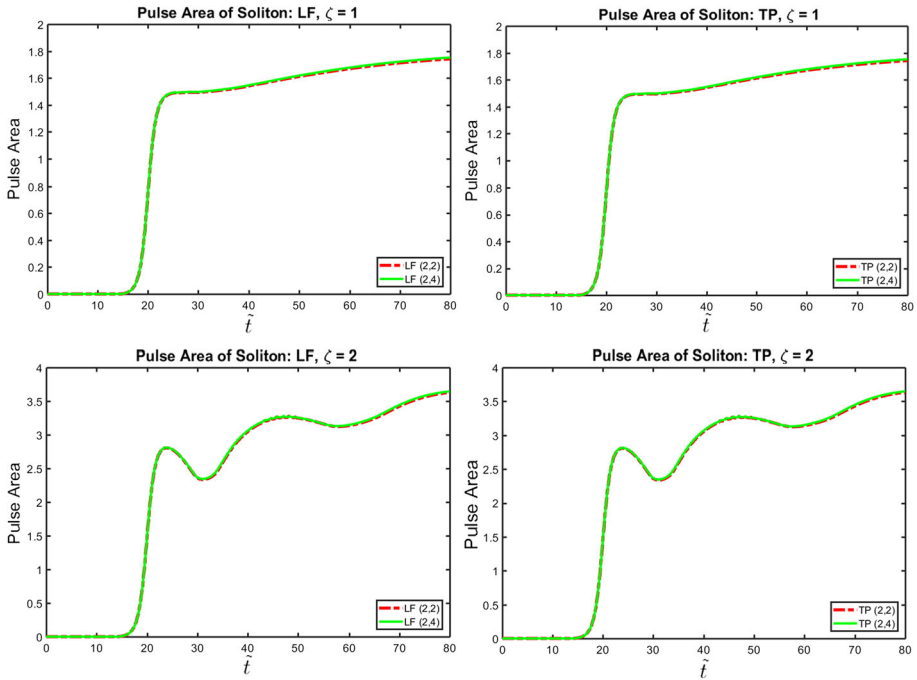


Fig. 6 Pulse area of transient fundamental ($\zeta = 1$, first row) and second order ($\zeta = 2$, second row) soliton propagation. First column: leap-frog FDTD scheme. Second column: trapezoidal FDTD scheme

Acknowledgements The authors would like to thank ICERM’s *Collaborate@ICERM* program as well as the *Research in Pairs* program at MFO, Oberwolfach in Germany for their support of co-authors Bokil, Cheng and Li.

Appendix A. $2M$ Order Spatial Discretizations

In this section, we provide a proof for Theorem 4.1 by following the exposition in [2, 6].

Proof Following the discussion in Sect. 4, assume that $u, v \in C_{\#}^{2m+3}([0, L])$ with $m \in \mathbb{N}$ an integer, and $m \geq 1$, where the subscript # is used to indicate periodic boundary conditions. Then, if $v_h \in V_{0,h}$ is a restriction of v to the primal grid and $u_h \in V_{\frac{1}{2},h}$ is a restriction of u to the dual grid, we have the following Taylor expansions [8, p.53]

$$\left(\tilde{\mathcal{D}}_h^{(2)} u_h\right)_\ell = \frac{\partial u}{\partial x}(x_\ell) + \sum_{i=1}^m \frac{h^{2i}}{(2i+1)!2^{2i}} \left(\frac{\partial^{2i+1} u}{\partial x^{2i+1}}\right)(x_\ell) + \mathcal{O}(h^{2m+2}), \tag{A.1}$$

$$\left(\mathcal{D}_h^{(2)} v_h\right)_{\ell+\frac{1}{2}} = \frac{\partial v}{\partial x}(x_{\ell+\frac{1}{2}}) + \sum_{i=1}^m \frac{h^{2i}}{(2i+1)!2^{2i}} \left(\frac{\partial^{2i+1} v}{\partial x^{2i+1}}\right)(x_{\ell+\frac{1}{2}}) + \mathcal{O}(h^{2m+2}). \tag{A.2}$$

By replacing $h/2$ by $(2p-1)h/2$ in (A.1) and by inserting the different Taylor expansions obtained from (A.1) into (4.8) with $m = M - 1$ we obtain ([8, p. 53])

$$\begin{aligned}
 \left(\tilde{D}_h^{(2M)} u_h\right)_\ell &= \sum_{p=1}^M \lambda_{2p-1}^{2M} \sum_{i=0}^{M-1} \left[\left(\frac{(2p-1)h}{2}\right)^{2i} \frac{1}{(2i+1)!} \left(\frac{\partial^{2i+1} u}{\partial x^{2i+1}}\right)(x_\ell) + \mathcal{O}(h^{2M}) \right] \\
 &= \sum_{i=0}^{M-1} \left[\frac{h^{2i}}{2^{2i}(2i+1)!} \left(\frac{\partial^{2i+1} u}{\partial x^{2i+1}}\right)(x_\ell) \sum_{p=1}^M \lambda_{2p-1}^{2M} (2p-1)^{2i} \right] + \mathcal{O}(h^{2M}).
 \end{aligned}
 \tag{A.3}$$

Requiring $\left(\tilde{D}_h^{(2M)} u\right)_\ell$ to approximate $\left(\frac{\partial u}{\partial x}\right)(x_\ell)$ with error $\mathcal{O}(h^{2M})$ leads to a system of equations in the coefficients λ_i^{2M} , for $i = 1, 2, \dots, 2M - 1$, given by

$$\begin{aligned}
 \lambda_1^{2M} + \lambda_3^{2M} &+ \lambda_5^{2M} + \dots + \lambda_{2M-1}^{2M} &= 1 \\
 \lambda_1^{2M} + 3^2 \lambda_3^{2M} &+ 5^2 \lambda_5^{2M} + \dots + (2M-1)^2 \lambda_{2M-1}^{2M} &= 0 \\
 \lambda_1^{2M} + 3^4 \lambda_3^{2M} &+ 5^4 \lambda_5^{2M} + \dots + (2M-1)^4 \lambda_{2M-1}^{2M} &= 0 \\
 \vdots & & \vdots \\
 \lambda_1^{2M} + 3^{2M-2} \lambda_3^{2M} &+ 5^{2M-2} \lambda_5^{2M} + \dots + (2M-1)^{2M-2} \lambda_{2M-1}^{2M} &= 0
 \end{aligned}
 \tag{A.4}$$

To solve system (A.4) and derive explicit formulas for the coefficients λ_i^{2M} , we rewrite system (A.4) in matrix form as

$$\begin{pmatrix} 1^0 & 3^0 & 5^0 & \dots & (2M-1)^0 \\ 1^2 & 3^2 & 5^2 & \dots & (2M-1)^2 \\ 1^4 & 3^4 & 5^4 & \dots & (2M-1)^4 \\ \vdots & & & & \\ 1^{2M-2} & 3^{2M-2} & 5^{2M-2} & \dots & (2M-1)^{2M-2} \end{pmatrix} \begin{pmatrix} \lambda_1^{2M} \\ \lambda_3^{2M} \\ \lambda_5^{2M} \\ \vdots \\ \lambda_{2M-1}^{2M} \end{pmatrix} = \begin{pmatrix} 1 \\ 0 \\ 0 \\ \vdots \\ 0 \end{pmatrix}.
 \tag{A.5}$$

Let the matrix of system (A.5) be denoted as W_{2M} . We define the vector $\lambda^{2M} = (\lambda_1^{2M}, \lambda_3^{2M}, \lambda_5^{2M}, \dots, \lambda_{2M-1}^{2M})^T$. Multiplying the linear system of equations in (A.5) by any vector $U = (U_1, U_2, \dots, U_M)^T \in \mathbb{R}^M$, we get the equation

$$U^T W_{2M} \lambda^{2M} = U_1.
 \tag{A.6}$$

Let $\mathcal{P} := \mathcal{P}_{2M-2}^{\text{even}}(\mathbb{R})$ be the set of all even polynomials of degree $2M - 2$ with real coefficients. Associated to the vector $U \in \mathbb{R}^M$, we define $P_U \in \mathcal{P}$ as

$$P_U(x) = U_1 + U_2(2x - 1)^2 + U_3(2x - 1)^4 + \dots + U_M(2x - 1)^{2M-2},
 \tag{A.7}$$

from which we obtain the equation

$$U^T W_{2M} = (P_U(1), P_U(2), P_U(3), \dots, P_U(M)),
 \tag{A.8}$$

which permits rewriting Eq. (A.6) as

$$\sum_{j=1}^M P_U(j) \lambda_{2j-1}^{2M} = P_U\left(\frac{1}{2}\right).
 \tag{A.9}$$

Satisfying Eq. (A.6) for any $U \in \mathbb{R}^M$ is equivalent to having Eq. (A.9) hold for any polynomial $P \in \mathcal{P}$.

For each integer $1 \leq p \leq M$, we now consider the polynomials in \mathcal{P} defined as

$$Q_p(x) = \prod_{1 \leq r \leq M, r \neq p} \left(1 - \frac{(2x - 1)^2}{(2r - 1)^2}\right),
 \tag{A.10}$$

The polynomial $Q_p(x)$ vanishes at all $x = 1, 2, 3, \dots, M$ except at $x = p$. Using $P = Q_p$ in (A.9) we have

$$Q_p(p)\lambda_{2p-1}^{2M} = Q_p\left(\frac{1}{2}\right) = 1,$$

which implies that

$$\lambda_{2p-1}^{2M} = \frac{1}{Q_p(p)} = \prod_{1 \leq r \leq M, r \neq p} \left(1 - \frac{(2p-1)^2}{(2r-1)^2}\right)^{-1}. \tag{A.11}$$

We use the following identities (given without proof)

$$\prod_{1 \leq r \leq M, r \neq p} \left(1 + \frac{(2p-1)}{(2r-1)}\right)^{-1} = \frac{2^p(p-1)!(2M-1)!!}{(2M+2p-2)!!}, \tag{A.12}$$

and

$$\prod_{1 \leq r \leq M, r \neq p} \left(1 - \frac{(2p-1)}{(2r-1)}\right)^{-1} = \frac{(-1)^{p-1}(2M-1)!!}{2^{p-1}(2M-2p)!!(2p-1)(p-1)!}, \tag{A.13}$$

where $p \in \mathbb{Z}, 1 \leq p \leq M$.

From Eqs. (A.11), (A.12) and (A.13), and some algebraic manipulations, we can obtain the explicit formula (4.10). □

Remark A.1 The result in (4.10) has been obtained, using other techniques, by other authors in the past (see [11], [15], and [12]). In [2], the authors prove several additional properties of the corresponding coefficients for higher order approximations of the 1D Laplace operator. Similar properties for the coefficients λ_{2p-1}^{2M} can be proved. Some of these properties have been proved in [15] and [12].

Appendix B. Symbol of the Operator \mathcal{A}_h

Following [4], we define $K = \frac{kh}{2}$, and use Chebyshev polynomial identities to get

$$\sin((2m-1)K) = \sum_{j=1}^m \alpha_j^m \sin^{2j-1}(K), \tag{B.1}$$

where, for $j = 1, 2, \dots, m$

$$\alpha_j^m := (-1)^{2m-j-1} \frac{2m-1}{m+j-1} \frac{(m+j-1)!}{(m-j)!} \frac{2^{2j-2}}{(2j-1)!}. \tag{B.2}$$

Using the identity (B.1) and rearranging terms, we obtain

$$\begin{aligned} \sum_{p=1}^M \frac{\lambda_{2p-1}^{(2M)}}{2p-1} \sin\left((2p-1)\frac{kh}{2}\right) &= \sum_{p=1}^M \frac{\lambda_{2p-1}^{(2M)}}{2p-1} \sum_{\ell=1}^p \alpha_\ell^p \sin^{2\ell-1}\left(\frac{kh}{2}\right) \\ &= \sum_{\ell=1}^M \left(\sum_{p=\ell}^M \frac{\lambda_{2p-1}^{(2M)}}{2p-1} \alpha_\ell^p\right) \sin^{2\ell-1}\left(\frac{kh}{2}\right). \end{aligned} \tag{B.3}$$

By definition of $\lambda_{2p-1}^{(2M)}$ and α_ℓ^p , we have

$$\sum_{p=\ell}^M \frac{\lambda_{2p-1}^{(2M)}}{2p-1} \alpha_\ell^p = \sum_{p=\ell}^M \frac{1}{2p-1} \frac{(-1)^{3p-\ell-2} 2^{2\ell-1} [(2M-1)!!]^2 (p+\ell-2)!}{(2M+2p-2)!! (2M-2p)!! (p-\ell)! (2\ell-1)!}. \tag{B.4}$$

Using the fact that $(2n)!! = 2^n n!$ and changing index from $p = j + \ell$ to index j , we get

$$\begin{aligned} \sum_{p=\ell}^M \frac{\lambda_{2p-1}^{(2M)}}{2p-1} \alpha_\ell^p &= \sum_{j=0}^{M-\ell} \frac{1}{(2j+2\ell-1)} \frac{(-1)^{3j+2\ell-2} 2^{2\ell-1} [(2M-1)!!]^2 (j+2\ell-2)!}{(2M+2j+2\ell-2)!! (2M-2j-2\ell)!! j! (2\ell-1)!} \\ &= \sum_{j=0}^{M-\ell} \frac{1}{2j+2\ell-1} \frac{(-1)^j 2^{2\ell-1} [(2M-1)!!]^2 (2\ell+j-2)!}{2^{M+j+\ell-1} (M+j+\ell-1)! 2^{M-j-\ell} (M-j-\ell)! j! (2\ell-1)!} \\ &= \frac{[(2M-1)!!]^2 2^{2\ell}}{2^{2M} (2\ell-1)!} \sum_{j=0}^{M-\ell} \frac{(-1)^j (2\ell+j-2)!}{(2j+2\ell-1)! (M+j+\ell-1)! (M-j-\ell)! j!}. \end{aligned}$$

Using the following recursion formulas, which we state without proof, for $n \in \mathbb{N}$,

$$\Gamma(n+1) = n\Gamma(n); \quad \text{with} \quad \Gamma\left(n + \frac{1}{2}\right) := \frac{(2n-1)!! \sqrt{\pi}}{2^n}, \tag{B.5}$$

we then have

$$\sum_{p=\ell}^M \frac{\lambda_{2p-1}^{(2M)}}{2p-1} \alpha_\ell^p = \frac{[(2M-1)!!]^2 2^{2\ell}}{2^{2M} (2\ell-1)!} \frac{[\Gamma(\ell - \frac{1}{2})]^2}{4[\Gamma(M + \frac{1}{2})]^2} = \frac{[(2\ell-3)!!]^2}{(2\ell-1)!}, \tag{B.6}$$

and

$$\sum_{p=1}^M \frac{\lambda_{2p-1}^{(2M)}}{2p-1} \sin\left((2p-1) \frac{kh}{2}\right) = \sum_{\ell=1}^M \frac{[(2\ell-3)!!]^2}{(2\ell-1)!} \sin^{2\ell-1}\left(\frac{kh}{2}\right). \tag{B.7}$$

References

1. Agrawal, G.P.: *Nonlinear Fiber Optics*. Academic Press, Cambridge (2007)
2. Anne, L., Joly, P., Tran, Q.H.: Construction and analysis of higher order finite difference schemes for the 1D wave equation. *Comput. Geosci.* **4**, 207–249 (2000)
3. Aregba-Driollet, D.: Godunov scheme for Maxwell’s equations with Kerr nonlinearity. *Commun. Math. Sci.* **13**, 2195–2222 (2015)
4. Bokil, V., Gibson, N.: Analysis of spatial high-order finite difference methods for Maxwell’s equations in dispersive media. *IMA J. Numer. Anal.* **32**, 926–956 (2012)
5. Bokil, V.A., Cheng, Y., Jiang, Y., Li, F.: Energy stable discontinuous Galerkin methods for Maxwell’s equations in nonlinear optical media. *J. Comput. Phys.* **350**, 420–452 (2017)
6. Bokil, V.A., Gibson, N.G.: High-order staggered finite difference methods for Maxwell’s equations in dispersive media. Technical Report ORST-MATH-10-01, Oregon State University. <http://hdl.handle.net/1957/13786>, January (2010)
7. Bourgeade, A., Nkongsa, B.: Numerical modeling of laser pulse behavior in nonlinear crystal and application to the second harmonic generation. *Multiscale Model. Simul.* **4**, 1059–1090 (2005)
8. Cohen, G.C.: *Higher-Order Numerical Methods for Transient Wave Equations*. Springer, Berlin (2001)
9. de La Bourdonnaye, A.: High-order scheme for a nonlinear Maxwell system modelling Kerr effect. *J. Comput. Phys.* **160**, 500–521 (2000)
10. Fisher, A., White, D., Rodrigue, G.: An efficient vector finite element method for nonlinear electromagnetic modeling. *J. Comput. Phys.* **225**, 1331–1346 (2007)

11. Fornberg, B.: On a Fourier method for the integration of hyperbolic equations. *SIAM J. Numer. Anal.* **12**(4), 509–528 (1975)
12. Fornberg, B., Ghrist, M.: Spatial finite difference approximations for wave-type equations. *SIAM J. Numer. Anal.* **37**, 105–130 (1999)
13. Fujii, M., Tahara, M., Sakagami, I., Freude, W., Russer, P.: High-order FDTD and auxiliary differential equation formulation of optical pulse propagation in 2-D Kerr and Raman nonlinear dispersive media. *IEEE J. Quantum Electron.* **40**, 175–182 (2004)
14. Gedney, S.D., Young, J.C., Kramer, T.C., Roden, J.A.: A discontinuous Galerkin finite element time-domain method modeling of dispersive media. *IEEE Trans. Antennas Propag.* **60**, 1969–1977 (2012)
15. Ghrist, M.: Finite Difference Methods for Wave Equations. Ph.D. Thesis, University of Colorado, Boulder, CO (2000)
16. Gilles, L., Hagness, S., Vázquez, L.: Comparison between staggered and unstaggered finite-difference time-domain grids for few-cycle temporal optical soliton propagation. *J. Comput. Phys.* **161**, 379–400 (2000)
17. Goorjian, P.M., Taflove, A., Joseph, R.M., Hagness, S.C.: Computational modeling of femtosecond optical solitons from Maxwell's equations. *IEEE J. Quantum Electron.* **28**, 2416–2422 (1992)
18. Greene, J.H., Taflove, A.: General vector auxiliary differential equation finite-difference time-domain method for nonlinear optics. *Opt. Express* **14**, 8305–8310 (2006)
19. Hile, C.V., Kath, W.L.: Numerical solutions of Maxwell's equations for nonlinear-optical pulse propagation. *JOSA B* **13**, 1135–1145 (1996)
20. Huang, Y., Li, J., Yang, W.: Interior penalty DG methods for Maxwell's equations in dispersive media. *J. Comput. Phys.* **230**, 4559–4570 (2011)
21. Ji, X., Cai, W., Zhang, P.: High-order DGTD methods for dispersive Maxwell's equations and modelling of silver nanowire coupling. *Int. J. Numer. Methods Eng.* **69**, 308–325 (2007)
22. Ji, X., Cai, W., Zhang, P.: Reflection/transmission characteristics of a discontinuous Galerkin method for Maxwell's equations in dispersive inhomogeneous media. *J. Comput. Mathematics Int. Edn.* **26**, 347 (2008)
23. Joseph, R.M., Hagness, S.C., Taflove, A.: Direct time integration of Maxwell's equations in linear dispersive media with absorption for scattering and propagation of femtosecond electromagnetic pulses. *Opt. Lett.* **16**, 1412–1414 (1991)
24. Joseph, R.M., Taflove, A.: Spatial soliton deflection mechanism indicated by FD–TD Maxwell's equations modeling. *IEEE Photon. Technol. Lett.* **6**, 1251–1254 (1994)
25. Joseph, R.M., Taflove, A.: FDTD Maxwell's equations models for nonlinear electrodynamics and optics. *IEEE Trans. Antennas Propag.* **45**, 364–374 (1997)
26. Joseph, R.M., Taflove, A., Goorjian, P.M.: Direct time integration of Maxwell's equations in two-dimensional dielectric waveguides for propagation and scattering of femtosecond electromagnetic solitons. *Opt. Lett.* **18**, 491–493 (1993)
27. Kashiwa, T., Fukai, I.: A treatment by the FD–TD method of the dispersive characteristics associated with electronic polarization. *Microwave Opt. Technol. Lett.* **3**, 203–205 (1990)
28. Kashiwa, T., Yoshida, N., Fukai, I.: A treatment by the finite-difference time domain method of the dispersive characteristics associated with orientational polarization. *IEEE Trans. IEICE* **73**, 1326–1328 (1990)
29. Kelley, D.F., Luebbers, R.J.: Piecewise linear recursive convolution for dispersive media using FDTD. *IEEE Trans. Antennas Propag.* **44**, 792–797 (1996)
30. Kinsler, P., Radnor, S., Tyrrell, J., New, G.: Optical carrier wave shocking: detection and dispersion. *Phys. Rev. E* **75**, 066603 (2007)
31. Lanteri, S., Scheid, C.: Convergence of a discontinuous Galerkin scheme for the mixed time-domain Maxwell's equations in dispersive media. *IMA J. Numer. Anal.* **33**, 432–459 (2013)
32. Li, J.: Error analysis of finite element methods for 3-D Maxwell's equations in dispersive media. *J. Comput. Appl. Math.* **188**, 107–120 (2006)
33. Li, J.: Error analysis of fully discrete mixed finite element schemes for 3-D Maxwell's equations in dispersive media. *Comput. Methods Appl. Mech. Eng.* **196**, 3081–3094 (2007)
34. Li, J., Chen, Y.: Analysis of a time-domain finite element method for 3-D Maxwell's equations in dispersive media. *Comput. Methods Appl. Mech. Eng.* **195**, 4220–4229 (2006)
35. Li, J., Huang, Y.: Time-domain finite element methods for Maxwell's equations in metamaterials, vol. 43. Springer, Berlin (2013)
36. Li, J., Shields, S.: Superconvergence analysis of Yee scheme for metamaterial Maxwell's equations on non-uniform rectangular meshes. *Numer. Math.* **134**, 741–781 (2016)

37. Luebbers, R., Hunsberger, F.P., Kunz, K.S., Standler, R.B., Schneider, M.: A frequency-dependent finite-difference time-domain formulation for dispersive materials. *IEEE Trans. Electromagn. Compat.* **32**, 222–227 (1990)
38. Luebbers, R.J., Hunsberger, F.: FDTD for Nth-order dispersive media. *IEEE Trans. Antennas Propag.* **40**, 1297–1301 (1992)
39. Monk, P., Süli, E.: A convergence analysis of Yee's scheme on nonuniform grids. *SIAM J. Numer. Anal.* **31**, 393–412 (1994)
40. Petropoulos, P.: Fourth-order accurate staggered finite difference schemes for the time-dependent Maxwell equations, in *Ordinary and partial differential equations*, Vol. V (Dundee, : vol. **370** of Pitman Res. Notes Math. Ser. Longman, Harlow 1997, pp. 85–107 (1996)
41. Prokopidis, K.P., Kosmidou, E.P., Tsiboukis, T.D.: An FDTD algorithm for wave propagation in dispersive media using higher-order schemes. *J. Electromagn. Waves Appl.* **18**, 1171–1194 (2004)
42. Ramadan, O.: Systematic wave-equation finite difference time domain formulations for modeling electromagnetic wave-propagation in general linear and nonlinear dispersive materials. *Int. J. Mod. Phys. C* **26**, 1550046 (2015)
43. Sørensen, M.P., Webb, G.M., Brio, M., Moloney, J.V.: Kink shape solutions of the Maxwell–Lorentz system. *Phys. Rev. E* **71**, 036602 (2005)
44. Taflove, A., Hagness, S.C.: *Computational Electrodynamics: The Finite-Difference Time-Domain method*, 3rd edn. Artech House, Norwood (2005)
45. Taflove, A., Oskooi, A., Johnson, S.G.: *Advances in FDTD Computational Electrodynamics: Photonics and Nanotechnology*. Artech House, Norwood (2013)
46. Tyrrell, J., Kinsler, P., New, G.: Pseudospectral spatial-domain: a new method for nonlinear pulse propagation in the few-cycle regime with arbitrary dispersion. *J. Mod. Opt.* **52**, 973–986 (2005)
47. Wang, B., Xie, Z., Zhang, Z.: Error analysis of a discontinuous Galerkin method for Maxwell equations in dispersive media. *J. Comput. Phys.* **229**, 8552–8563 (2010)
48. Xie, Z., Chan, C., Zhang, B.: An explicit fourth-order staggered finite-difference time domain method for Maxwell's equations. *J. Comput. Appl. Math.* **147**, 75–98 (2002)
49. Yee, K.: Numerical solution of initial boundary value problems involving Maxwell's equations in isotropic media. *IEEE Trans. Antennas Propag.* **14**, 302–307 (1966)
50. Yefet, A., Petropoulos, P.G.: A fourth-order FD-TD scheme for electromagnetics, in *Mathematical and numerical aspects of wave propagation* (Santiago de Compostela, 2000), SIAM, Philadelphia, PA, pp. 883–887 (2000)
51. Yefet, A., Petropoulos, P.G.: A staggered fourth-order accurate explicit finite difference scheme for the time-domain Maxwell's equations. *J. Comput. Phys.* **168**, 286–315 (2001)
52. Young, J., Gaitonde, D., Shang, J.: Toward the construction of a fourth-order difference scheme for transient EM wave simulation: staggered grid approach. *IEEE Trans. Antennas Propag.* **45**, 1573–1580 (1997)
53. Young, J.L., Nelson, R.O.: A summary and systematic analysis of FDTD algorithms for linearly dispersive media. *IEEE Antennas Propag. Mag.* **43**, 61–77 (2001)
54. Young, L.: A higher order FDTD method for EM propagation in a collisionless cold plasma. *IEEE Trans. Antennas Propag.* **44**, 1283–1289 (1992)
55. Zhu, B., Chen, J., Zhong, W., Liu, Q.: A hybrid finite-element/finite-difference method with an implicit-explicit time-stepping scheme for Maxwell's equations. *Int. J. Numer. Modell. Electron. Netw. Dev. Fields* **25**(5–6), 607–620 (2012)
56. Ziolkowski, R.W., Judkins, J.B.: Nonlinear finite-difference time-domain modeling of linear and nonlinear corrugated waveguides. *JOSA B* **11**, 1565–1575 (1994)